



Master Thesis

A Hedgerow chronosequence: SOC sequestration potentials and persistence in cultivated soils of Lower Austria

submitted by

Frederik Nygaard Philipsen, BSc.

in the framework of the international Master programme

Environmental Sciences – Soil, Water and Biodiversity

in partial fulfilment of the requirements for the academic degree

Master of Science

Vienna, May 2022

Co-Supervisor:

Assoc.Prof. Bjarne W. Strobel
Section for Environmental Chemistry & Physics
Dept. of Plant and Environmental Sciences
University of Copenhagen

Main Supervisor:

Univ.-Prof. Dr. Walter W. Wenzel
Institute of Soil Research
Dept. of Forest- and Soil Sciences
Univ. of Natural Resources and Life Science, Vienna

Affidavit

I hereby declare that this master thesis is my own work, without any unpermitted assistance from third parties. I confirm that no sources have been used other than those explicitly referenced in the text.

I further declare that this mater thesis has not been submitted, in whole or in part, in the same or similar form, to any other educational institution as part of the requirements for an academic degree.

Vienna, May 2022

Frederik Nygaard PHILIPSEN

A handwritten signature in blue ink, appearing to read "Fred Nyg.", enclosed in a light blue rectangular box.

Acknowledgements

Thanks to everyone who took part in and made this work possible, from development to finishing. I would like to thank my main supervisor Walter Wenzel, for being the voice of reason throughout the process and providing many valuable insights. Thanks to my co-supervisor Bjarne Strobel for exciting discussions and for always being a source of optimism.

I am also very grateful for all the help in work and in spirit, I received from the Rhizo Group in Tulln with a special thanks to Philipp De Jong and Monika Laux for the support during the many hours by the sieves in the “Plant Lab”. Also, thanks to Lauren Herold, Lisa Stein, and Joanne O’Keeffe for helping in the field.

Lastly, thanks to Sarah, family, and friends for all your support.

Table of contents

Affidavit	ii
Abstract	vi
Zusammenfassung	vii
1. Introduction and objectives	1
1.1 SOC stock development	1
1.2 Hedgerows	2
1.3 SOC persistence	3
1.4 Objectives and hypotheses	6
2. Materials and Methods	7
2.1 Study area	7
2.2 Study design and sampling	9
2.3 Particle size SOC fractionation	12
2.4 pH	15
2.5 SOC calculations	15
2.6 C_{sat} and C_{def}	18
2.7 Statistical analyses	19
3. Results	20
3.1 Basic soil properties	20
3.2 SOC stock calculation methods	22
3.3 SOC stocks in bulk soil (< 2000 µm)	24
3.4 SOC in particle size fractions	25
3.5 SOC sequestration over time	29
3.6 C_{sat} and C_{def}	33
4. Discussion	36
4.1 Depth distribution of SOC	36
4.2 SOC sequestration in bulk soil	37
4.3 SOC sequestration in particle size fractions	40
4.4 C_{sat} and C_{def}	42
4.5 Implications of C_{sat} model choice	44

4.5 Hedgerow planting as climate change mitigation.....	45
5. Concluding remarks	48
6. References.....	50
7. Abbreviations	57
8. List of Figures	58
9. List of Tables.....	60
10. Appendices.....	61

Abstract

Changes in soil organic carbon (SOC) stocks can affect atmospheric CO₂ concentrations, soil nutrient cycling, and water-holding capacity. To increase SOC, reforestation, integration of agroforestry elements in SOC-depleted cropland soils may serve as potential means for SOC sequestration. However, SOC varies in persistence, and it is recognized that the fine SOC fraction ($f_{<20\ \mu\text{m}}$) associated with mineral particles and microaggregates are more persistent than large, free fractions ($f_{>20\ \mu\text{m}}$). Since the proportion of $f_{<20\ \mu\text{m}}$ can become saturated, knowledge of its saturation level and developments over time is important to evaluate the feasibility of increasing persistent SOC storage. In this master thesis, a space-for-time substitution approach was employed based on a hedgerow chronosequence (1950-2019) and adjacent agricultural fields in Lower Austria. By selecting 13 proximate sites in the Pannonian region, the aim was to simulate decadal-scale changes in SOC-fractions in cultivated soil after hedgerow planting. Particle size fractionation via ultrasonic aggregate dispersion and sequential wet sieving was performed to analyze the temporal dynamics of hedgerow induced SOC sequestration, and its partitioning into size fractions.

The results showed that hedgerows significantly sequestered SOC in 0-20 cm – equal to a sequestration rate of 0.48 t C ha⁻¹ in bulk soil, while no effects were observed in 20-40 cm. SOC was mainly stored in $f_{<20\ \mu\text{m}}$ for both land uses, however SOC $f_{>20\ \mu\text{m}}$ constituted a larger proportion of hedgerow topsoil. While SOC enrichment under hedgerows took place in all size fractions, SOC in $f_{>20\ \mu\text{m}}$ showed a stronger relationship with hedgerow age than in $f_{<20\ \mu\text{m}}$. Modelling carbon saturation potentials revealed that soils were generally far from saturation, indicating a large unused storage potential, though hedgerows slightly increased saturation levels. Overall, hedgerows can contribute to SOC sequestration in the study area, however more data is needed to verify the trends observed.

Zusammenfassung

Änderungen in den Beständen an organischem Kohlenstoff (SOC) im Boden können die atmosphärischen CO₂-Konzentrationen, den Nährstoffkreislauf und die Wasserhaltekapazität beeinflussen. Um den SOC zu erhöhen, können die Wiederaufforstung und die Integration von agroforstwirtschaftlichen Elementen in SOC-verarmten Ackerlandböden als potenzielle Mittel zur Sequestrierung von SOC dienen. Der SOC variiert jedoch in der Persistenz, und es ist anerkannt, dass feine SOC-Fractionen ($f_{<20 \mu m}$), die mit Mineralpartikeln und Mikroaggregaten verbunden sind, persistenter sind als partikuläre, freie Fractionen ($f_{>20 \mu m}$). Da der Anteil von $f_{<20 \mu m}$ gesättigt werden kann, ist die Kenntnis seines Sättigungsgrades und seiner zeitlichen Entwicklung wichtig, um die Machbarkeit einer Erhöhung der persistenten SOC-Speicherung zu bewerten. Basierend auf einer Heckenchronosequenz (1950-2019) und angrenzenden landwirtschaftlichen Flächen in Niederösterreich wurde ein Raum-für-Zeit-Substitutionsansatz verwendet. Durch die Auswahl von 13 Nachbarstandorten auf Schwarzerdeböden in der trockenen pannonischen Region war das Ziel, die Veränderungen der SOC-Fractionen unterschiedlicher Persistenz über einen Zeitraum von 70 Jahren nach der Heckenpflanzung zu simulieren. Partikelgrößenfraktionierung mittels Ultraschall-Aggregatdispersion und sequenzielle Nasssiebung wurde durchgeführt, um die zeitliche Dynamik der heckeninduzierten SOC-Sequestrierung und ihre Aufteilung in Größenfraktionen zu analysieren. Hecken sequestrierten SOC signifikant in 0–20 cm – das entspricht einer Sequestrierungsrate von 0.48 t C ha⁻¹, während in 20–40 cm keine Auswirkungen beobachtet wurden. SOC wurde hauptsächlich in $f_{<20 \mu m}$ für beide Landnutzungen gespeichert, jedoch machte SOC $f_{>20 \mu m}$ einen größeren Anteil im Heckenoberboden aus. Während die SOC-Anreicherung unter Hecken in allen Größenfraktionen stattfand, zeigte der SOC in $f_{>20 \mu m}$ eine stärkere Beziehung zum Heckenalter als in $f_{<20 \mu m}$. Die Modellierung von Kohlenstoffsättigungspotenzialen und -defiziten ergab, dass Hecken die Sättigungsdefizite leicht verringerten, die Böden jedoch im Allgemeinen weit von der Sättigung entfernt waren, was auf ein großes ungenutztes Speicherpotenzial hinweist. Insgesamt können Hecken zur SOC-Sequestrierung im Untersuchungsgebiet beitragen, es sind jedoch weitere Daten erforderlich, um die beobachteten Trends zu verifizieren

1. Introduction and objectives

Soils are foundational to the sustainability of terrestrial ecosystems including functions that ensure basic human needs, such as food security and clean water (Keesstra et al., 2016). Soil organic matter (SOM) is an essential component of soil providing a wide range of benefits related to nutrient availability, water holding capacity and soil structure (Blume et al., 2016a). Global SOM stocks also contain the largest terrestrial pool of organic carbon (OC) approx. 1400-1600 Pg in the upper meter of soil, which is twice as much as the 867 Pg carbon (C) estimated to be present in the atmosphere (Batjes, 2014; Lal, 2018). Human disturbances of the pedosphere by conversion of natural ecosystems into managed ones, have made soils net sources of CO₂ to the atmosphere over the past millennia (Sanderman et al., 2017). Estimates of historic SOC losses have been approximated to be 115-154 Pg C, which amounts to around 10% of current stocks (Lal, 2018). Thus, future changes in the world's soil organic carbon (SOC) stocks can cause substantial climate feedbacks if soils act as net sinks or sources of CO₂ to the atmosphere. With still increasing growth rates of atmospheric CO₂ concentrations, there is an urgent need for reducing greenhouse gas (GHG) emissions within the next decade in order to restrict climate warming to 1.5 °C above preindustrial levels, as stipulated in the Paris Agreement (Millar et al., 2017; Friedlingstein et al., 2020). Therefore, the potential to replenish global SOC stocks to mitigate radiative forcing has received much attention in the scientific community as well as in public climate policies e.g., the '4 per 1000 initiative' established during COP21 in 2015 (Minasny et al., 2017). While most of the scientific community agree that SOC stocks can be increased, the magnitude of accrual and its effect on atmospheric CO₂ levels is still debated (de Vries, 2018; Minasny et al., 2018; VandenBygaart, 2018).

1.1 SOC stock development

For the purposes of increasing SOC stocks to compensate for CO₂-emissions from the agricultural sector or other anthropogenic sources, a distinction between *sequestration* and *storage* of SOC, often used interchangeably, has been proposed (Chenu et al., 2019; Olson et al., 2014). While SOC storage refers to the accrual of SOC stocks in a defined land unit over time, SOC sequestration entails transferring atmospheric CO₂ into a defined land unit of soil over time through organic matter (OM) stored as SOM (Chenu et al., 2019). A result of this distinction is that external OC inputs (photosynthetically assimilated outside the land unit of concern) such as manure, compost, biochar or SOM deposited by wind and water,

should be considered a redistribution of SOC storage rather than SOC sequestration (Olson et al., 2014). Thus, SOC sequestration by increasing OC inputs is limited to that which can be photosynthesized within a land unit.

SOC stock development is a function of OC inputs and the rate of C losses (Chenu et al., 2019). If these become constant over time, SOC stocks will eventually reach a steady-state. Changes in inputs or outputs can cause SOC stocks to exit its steady-state and eventually reach a new one – higher or lower than the previous equilibrium. Thus, low return of OM, high decomposition, and vulnerability to leaching and erosion associated with soils under cultivation have led to SOC stock depletion from a previously higher steady-state (Lal, 2004; Wiesmeier et al., 2019). Numerous measures to restore cultivated SOC stocks through either increasing inputs or reducing losses have been studied. Farmers can increase C inputs by enhancing plant productivity through liming, irrigation and fertilization (Lemke et al., 2010; Paradelo et al., 2015), by crop residue incorporation, and by crop diversification measures such as deeply rooted crops, cover crops and agroforestry (Poeplau and Don, 2015; Wiesmeier et al., 2019). External sources of C may also be added, including biochar, compost and manure (Weng et al., 2017; Poulton et al., 2018). Reduction of C losses may be achieved through minimization of decomposition through less intensive tillage operations and reducing erosion risks through cover crops and hedgerow vegetation (Tiefenbacher et al., 2021). This thesis will specifically investigate the SOC sequestration potentials of hedgerows in agricultural soils.

1.2 Hedgerows

Hedgerows are historically important landscape features in many parts of Europe, originally planted as property boundaries and additional sources of fuel and food (Baudry et al., 2000; Holden et al., 2019). While diverse in both composition and management, a hedgerow may generally be defined as “*a linear feature composed of shrubs and/or trees that forms part of a management unit*” (Baudry et al., 2000, p. 8). Hedgerows have been in decline during the second half of the 20th century as their original functions became obsolete following agricultural intensification (McCann et al., 2017). In England and Wales, more than a million kilometers of hedgerows have been lost since 1945 (O’Connell et al., 2004) and current hedgerow networks in Belgium constitute just 30% of the extent in 1960 (Van Den Berge et al., 2021).

Concurrent with the accumulating body of evidence documenting the substantial effects of agricultural expansion and intensification on habitats, biodiversity, carbon storage and soil fertility the provision of ecosystem services by hedgerows have become increasingly acknowledged (Foley et al., 2011). Hedgerows have been shown to constitute important habitats for birds and insects (Laura et al., 2017; Heath et al., 2017), increase plant species richness (Haddaway et al., 2018), filter nutrients and contaminants (Holden et al., 2019; Weninger et al., 2021), reduce risks of erosion (Haddaway et al., 2018) and increase above- and belowground C stocks (Axe et al., 2017; Drexler et al., 2021). Subsequently, hedgerows have been increasingly protected by environmental legislation (Baudry et al., 2000) and included in agri-environmental schemes to promote replanting – recently as part of EU Biodiversity Strategy for 2030 (European Commission, 2021).

Soils under hedgerows or comparable agroforestry systems generally store more SOC than soils under cultivation (Lorenz & Lal, 2014; De Stefano & Jacobson, 2017; Drexler et al., 2021; Mayer et al., 2022). Woody hedgerow vegetation enhances root-derived C inputs through extensive and deep root-systems, shown to be more important for SOM formation than shoot-derived C (Lorenz & Lal, 2014). Losses of C are reduced since hedgerows are not harvested like croplands, though trimming and coppicing of hedgerows occurs depending on regional traditions and specific functions (Baudry et al., 2000). Furthermore, SOC losses are prevented under hedgerows due to protection from soil erosion and microclimatic conditions such as higher soil moisture and lower soil temperatures, resulting in decreased decomposition rates compared to adjacent arable soils (Van Den Berge et al., 2021). The effects of hedgerow age on SOC stocks are not consistent in the scientific literature. Biffi et al. (2022) provide evidence that SOC sequestration under hedgerows in the UK increase as a function of age, while others have been unable to report such relationships (Ford et al., 2019). A recent review article by Drexler et al. (2021) suggests that hedgerows may enhance SOC especially within the first 20 years. Such gains are, however, expected to reach a steady-state after approx. 50 years when trees and shrubs reach maturity (Drexler et al., 2021). Moreover, as hedgerows provide OC inputs to soils directly from atmospheric CO₂, the SOC stock increases can be considered SOC sequestration cf. Olson et al. (2014).

1.3 SOC persistence

An important nuance of increasing SOC stocks to offset CO₂-emissions to the atmosphere is how persistent SOC will be once it is stored. That is, SOC residing in soils for long, will delay its release as

CO₂. SOC is stored in SOM that may persist in soil from one year to more than a millennium (von Lützow et al., 2006). The stabilizing mechanisms determining the fate of SOM has been studied extensively and several authors have summarized its primary mechanisms (Dynarski et al., 2020; Lehmann and Kleber, 2015; Six et al., 2002; von Lützow et al., 2006). Six et al. (2002) proposed three main stabilization mechanisms: (1) *Chemical stabilization*, occurring when OM adsorbs to clay and silt particles thus limiting bioavailability to soil microbes. (2) *Physical protection* from decomposition especially within stable microaggregates as OM becomes physically inaccessible to decomposers and (3) *biochemical stabilization* relating to the inherent recalcitrance of OM, caused e.g., by covalent bonds and aromaticity (Six et al., 2002). While biochemical stabilization was formerly viewed as the most decisive stabilizing mechanism, novel dating techniques (¹³C tracer analyses and ¹⁴C dating) have shown that the most persistent SOM are labile compounds associated with mineral surfaces (Han et al., 2016; Kleber et al., 2011). A comprehensive synthesis of existing hypotheses, highlighting the importance of mineral surfaces and aggregation as primary protection mechanisms was proposed by Lehmann & Kleber (2015) in their *Soil Continuum Model* (SCM, see Figure 1.1). SCM proposes that SOM exists as a continuum of organic fragments of different origin that are continuously broken down by decomposers into smaller and smaller parts. As SOM is depolymerized, dissolved and reiteratively processed by the microbial community, its protection by soil minerals and microaggregate formation becomes larger due to increased chemical reactivity (Lehmann and Kleber, 2015). The fraction of low molecular size and weight SOM protected by mineral particles is known as mineral-associated organic matter (MAOM) and has been proposed to persist in soils from decades to centuries (von Lützow et al., 2006). In contrast, SOM existing as litter or large biopolymers “further up the ladder” of the soil continuum (Figure 1.1) are less protected and termed particulate organic matter (POM) and has been suggested to have turnover time of years to decades (von Lützow et al., 2006). Protection of POM is thus more reliant on biochemical stabilization and occlusion in macroaggregates (Six et al., 2002). While POM is less persistent than MAOM, it still contributes to many important soil functions such as nutrient cycling, structural stability, and substrate for the microbial community (Chenu et al., 2019). Fundamental differences between MAOM and POM have made them relevant fractions to distinguish between, particularly when trying to

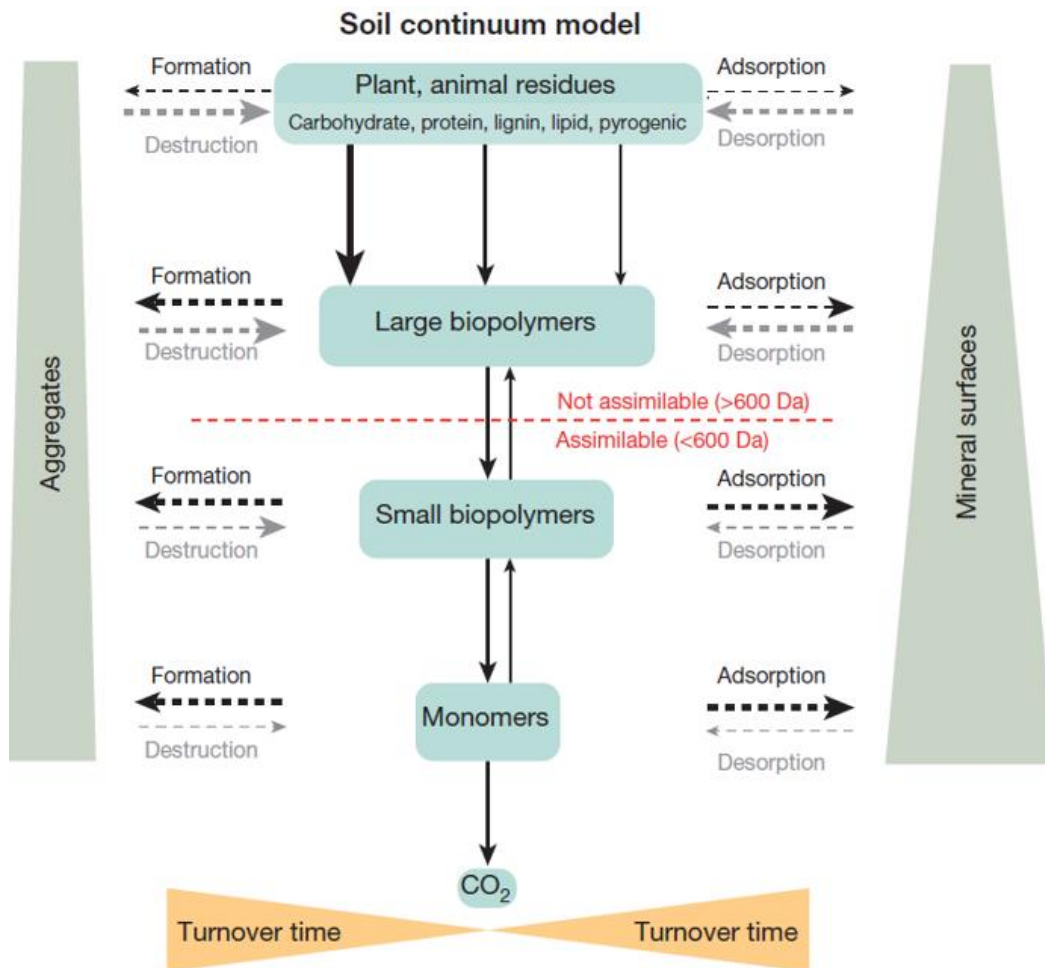


Figure 1.1 Soil continuum model (Lehmann & Kleber, 2015). All arrows illustrate processes dependent on temperature, moisture, and present biota. Dashed arrows represent mainly abiotic transfers while solid lines denote mainly biotic transfers. Thicker lines illustrate fast rates; large boxes and end of wedges illustrate bigger pool sizes.

predict the persistence of SOC in soil (Lavallee et al., 2019). Such separation can be achieved through physical fractionation procedures based on particle size, density or both (von Lützow et al., 2007).

While POM is thought to accumulate as a function of in- and output of OM, MAOM can reach a point of saturation. This was observed by Hassink (1997) who found that SOC concentrations in the silt- and clay sized fraction of soil $<20 \mu\text{m}$ ($f_{<20 \mu\text{m}}$) was positively correlated with the proportion of mineral particles in $f_{<20 \mu\text{m}}$. Thus, Hassink proposed that the capacity of soil to stabilize SOC in MAOM (here represented by SOC in $f_{<20 \mu\text{m}}$) is dependent on soil texture, namely that fine-textured soils with a large proportion of mineral particles in $f_{<20 \mu\text{m}}$ will have a larger protective capacity than coarse-textured soils

dominated by mineral particles larger than 20 μm . Hassink derived an equation to predict a soil's protective capacity based on soils under natural vegetation, assumed to be near saturation. This was later termed the carbon saturation potential (C_{sat}) (Angers et al., 2011). Estimations of C_{sat} and how far soils are from saturation may help inform management efforts about where additional persistent $f_{<20\ \mu\text{m}}$ SOC has the largest potential to be stored and help predict the role of soils in the GHG budget.

1.4 Objectives and hypotheses

The main objective of this master's thesis was to investigate the contribution of perennial hedgerow vegetation to SOC sequestration and by space-for-time-substitution, model its temporal dynamics over 70 years in Lower Austrian soils under cultivation. Furthermore, particular interest was on the persistence of prospective SOC sequestration, assessed by the partitioning of SOC into different particle size fractions. Drawing on an extensive soil sampling campaign of soil under hedgerows planted between 1950 and 2019 and adjacent cultivated soils (119 sites) by Herold (2022), a sample subset (13 sites) was selected for further investigation. Subsequently, a particle size fractionation procedure was employed to separate MAOM, operationally defined as SOC in $f_{<20\ \mu\text{m}}$ and POM represented by SOC in two size fractions: $f_{200-20\ \mu\text{m}}$ and $f_{2000-200\ \mu\text{m}}$.

The following hypotheses were posited:

(H1) Bulk SOC stocks (in $f_{<2000\ \mu\text{m}}$) under hedgerows will increase concurrent with hedgerow age compared to the baseline of adjacent soils under cultivation.

(H2) SOC in $f_{<20\ \mu\text{m}}$ under hedgerows will increase concurrent with hedgerow age compared to the baseline of adjacent soils under cultivation if hedgerow soils do not reach saturation.

2. Materials and Methods

2.1 Study area

The study area comprises of 13 paired hedgerow-field sites in the federal province of Lower Austria in NE Austria. Using a centroid on 48°30'54.7 N, 16°33'18.9 E, all sites were within a radius of 45 km distributed over the Lower Austrian districts of Mistelbach, Gänserndorf and Hollabrunn (Figure 2.1).

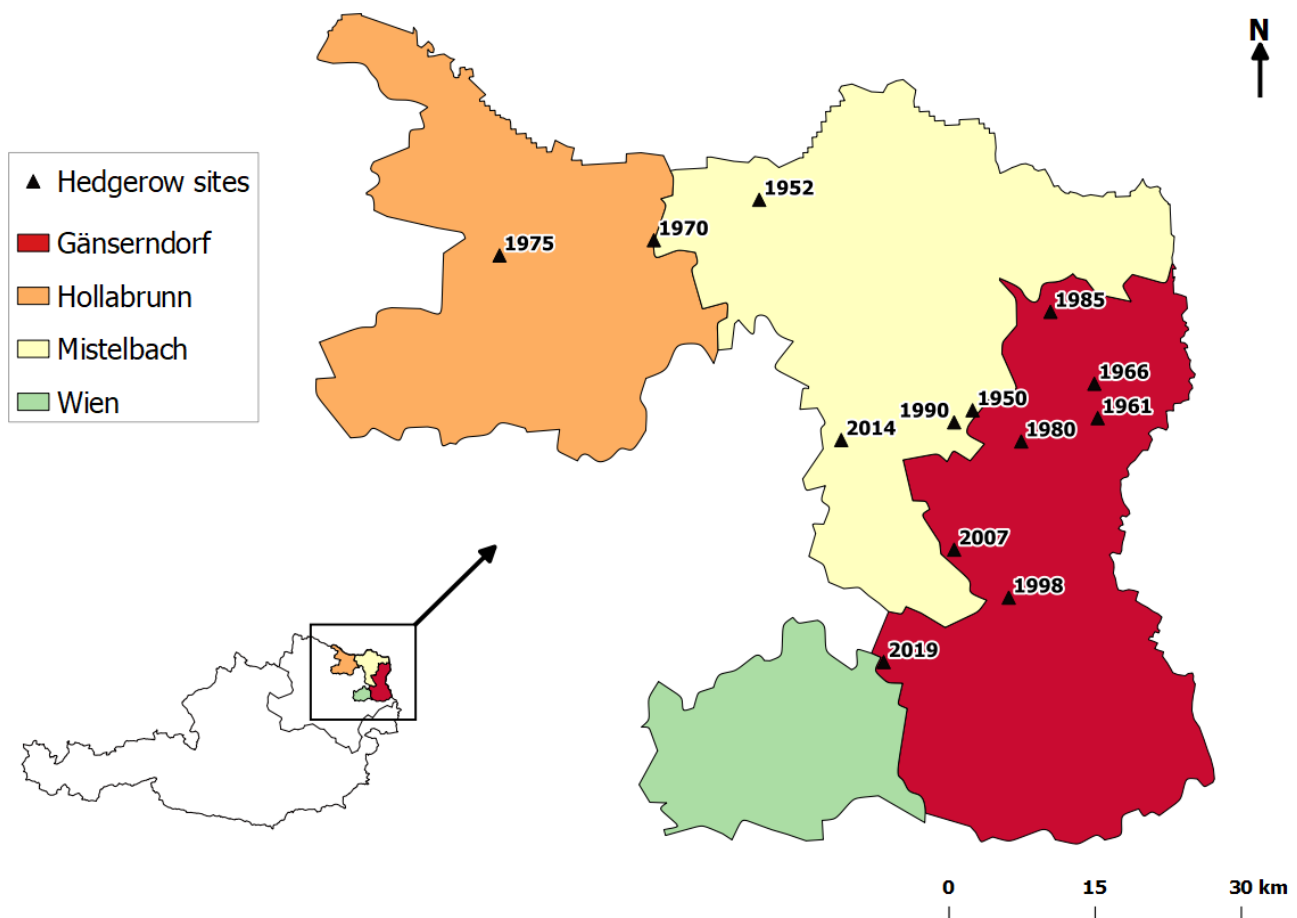


Figure 2.1 Map of sampling sites and their locations within Lower Austrian districts of the study area (Own work made in QGIS 2.18. using geodata from Statistics Austria (2020)).

The studied districts are located in the NE, Pannonian part of Lower Austria in the so-called “dry loess landscape” characterized by climatic continentality provided by the Bohemian Massif to the west and the alps in the south. This ‘continental shielding’ limits moisture influences from the Atlantic Ocean and

Mediterranean Sea which accommodates lower precipitation compared to western parts of Lower Austria (Sprafke et al., 2013). Mean annual precipitation and air temperature was 513 mm and 9.4°C respectively for the climate period 1981-2010 (Zentralanstalt für Metrologie und Geodynamik, 2021).

All studied soils are classified as Tschernosem according to the Austrian Soil Taxonomy which main diagnostic feature is a thick, blackish, humus-rich (SOM-rich) A-horizon (≥ 30 cm) with carbonate and silicate-rich fine sediments as parent material (Nestroy et al., 2011). The Austrian classification is less discriminative than the FAO World Reference Base for Soil Resources (WRB) which is evident in that Tschernosem is not directly equivalent to the reference soil group *Chernozem*, but also cover *Phaeozem* and occasionally *Kastanozem* groups in the WRB (Nestroy et al., 2011). The three WRB groups mainly differ in color as Chernozems have darker topsoil than Kastanozems and Phaeozems have lower base saturation and contain no secondary carbonates in topsoil (IUSS Working Group WRB 2015).

Loess is the dominant soil parent material in the study area resulting from deposits in NE Lower Austria, transported with glacial meltwater from aeolian deposits in Northern Europe through the Moravian Depression into this part of the Danube Basin during the most recent Pleistocene glaciation (Smalley and Leach, 1978). Loess is generally defined as having particle sizes between 63-6.3 μm consisting mainly of quartz, feldspar and mica minerals as well as a variable fraction of CaCO_3 (Haase et al., 2007). Texture classes in the studied sites were predominately loamy silt, which reflects the widespread presence of loess as parent material. As a growth medium for plants, loess provides optimal conditions in terms of water retention and root penetration with medium pore sizes (Blume et al., 2016b). Thus, climatic conditions coupled with high fertility loess derived Tschernosem, and a rather flat terrain has pathed the way for intensive cultivation in this region of Lower Austria. Accordingly, arable land is by far the most dominant land use in the study area with grasslands occurring sporadically (Wenzel et al., 2022).

Although long-term management history was not investigated, the predominant crop types planted in the growing season after soil sampling (July 2021) were cereals (*Triticum*, *Hordeum*) while a few fields also cultivated squash (*Cucurbita pepo*) and sunflower. Hedgerow vegetation was dominated by a few species of shrubs (*Ligustrum vulgare*, *Rhamnus cathartica* and *Rosa canina*) and tree species such as wild cherry (*Prunus avium*) and European ash (*Fraxinus excelsior*). However, many of the 33 identified species (in 11 sites) were only found in one site.

2.2 Study design and sampling

This study was designed to test the effects of hedgerows as soil treatments by comparison with cultivated soils that functioned as control treatments or, in the context of SOC sequestration, the pre-treatment baseline SOC. Hedgerow and control treatments were replicated to represent SOC sequestration potentials of hedgerows *in-situ* in the agricultural landscape of the study area. As already described, SOC sequestration is a process that happens over time, and knowledge of its temporal dynamics is essential to make reliable predictions about its impact on atmospheric CO₂-levels (Chenu et al., 2019). Ideally, direct, and repeated observations of such temporal changes in a site would be carried out, however such monitoring programs are rare and both expensive in terms of time and resources. Therefore, indirect strategies are often employed to reconstruct long-term changes in soil and vegetation. This study establishes a *chronosequence*, i.e., a series of sites that were formed under similar conditions (parent material, substrate), but differ in the time since they were formed (Walker et al., 2010). By assuming that younger sites follow the same trajectory as older sites, a so-called *space-for-time-substitution* approach

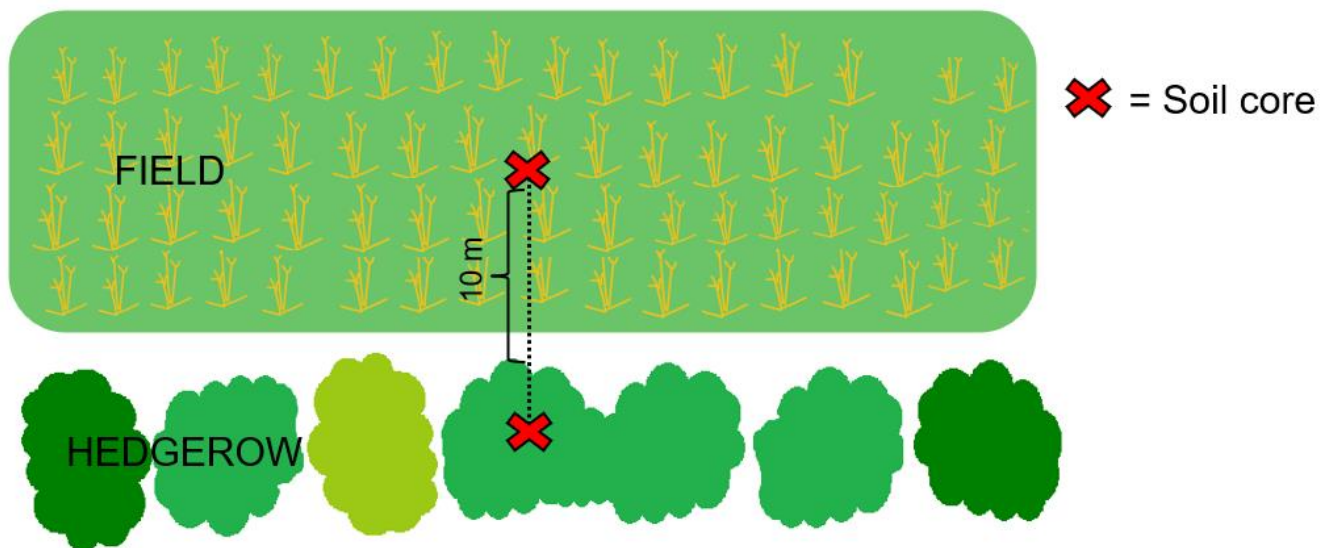


Figure 2.2 Soil sampling schematic for soil cores drawn from under hedgerows and adjacent field under cultivation (own work).

allowed the study of how spatially separated sites evolved over time as if they had occurred on the same site (Walker et al., 2010). This assumption rests on the notion of similar forming conditions. The sample material used in this study was based on the work of Professor Walter W. Wenzel & M.Sc. Lauren Herold

(Institute of Soil Research, BOKU), who initiated a project in collaboration with the Lower Austrian Landscape Fond (LAFO) to investigate the provision of ecosystem services by hedgerows in Lower Austrian agroecosystems. To meet this end, 119 field-bordering hedgerows with recorded planting years were selected through the Lower Austrian agricultural district authority's databases cross referenced with the federal Digital Soil Map (eBod). Sites were selected based on geographical proximity within the Pannonian region of Lower Austria, similar soil type and evenly distributed across the hedgerow age range (1-70 years). Selected sites were sampled between December 2019 and January 2020 under both hedgerows and adjacent fields under cultivation. Soil cores were drawn with a Ø-5 cm auger to a depth of 40 cm and then divided in two 20 cm increments (0-20 cm and 20-40 cm) in the field to distinguish between top- and subsoil in later analyses. Once a soil core was pulled out from under a hedge, a field sample was taken 10 meters from the hedgerow edge on the field (see Figure 2.2). Where grass strips occurred between hedgerow and field, the 10 meters were measured from the strip-field boundary. The 10-meter distance is based on results reported by others suggesting that hedgerow effects on SOC are negligible outside a 4-meter radius (Ford et al., 2019). Upon sampling and labelling samples were sieved to 2000 µm and air-dried.

The 13 sites analyzed in this study, were selected as a subset of the 119 sites collected as part of the LAFO project (Table 2.1). Sites were selected according to the same criteria as stated above, however representing only Tschernosem soils. The 1–70-year age range was preserved by selecting sites with hedgerow ages as evenly distributed as possible. Age differences between hedgerow sites ranged between 2-9 years with an average age interval of 6 years. For later analysis of hedgerow age effects, sites were categorized according to age within three groups: 1-22 years (1, 6, 13, 22), 30-45 years (30, 35, 40, 45) and 50-70 years (50, 54, 59, 68 and 70).

Table 2.1 Overview of the selected sites investigated in this study. NÖ = Lower Austria. Texture classes were translated from Austrian textural classification to FAO guidelines for soil description (Jahn et al., 2006).

Age group [y]	Hedgerow age [y]	NÖ district	Texture class (FAO)	Hedgerow species
50-70	70	Mistelbach	Silt loam	<i>C. mas, C. avellana, C. monogyna, P. domestica</i>
	68	Mistelbach	Sandy loam	<i>F. excelsior, R. pseudoacacia</i>
	59	Gänserndorf	Silt loam	<i>A. platanoides, F. excelsior, P. nigra, P. avium, Q. robur, S. nigra, S. aucuparia, S. vulgaris</i>
	54	Gänserndorf	Silt loam	NA
	50	Mistelbach	Silt loam	<i>A. negundo, L. vulgare, R. cathartica</i>
30-45	45	Hollabrunn	Sandy loam	<i>A. negundo, A. pseudoplatanus</i>
	40	Gänserndorf	Silt loam	<i>A. negundo, E. europaeus, F. excelsior, L.vulgare, R. cathartica,, R. pseudoacacia, R. canina</i>
	35	Gänserndorf	Silt loam	<i>C. arborescens, C. monogyna, F. excelsior, P.domestica, P. communis, R. cathartica, R. canina, S. nigra</i>
	30	Mistelbach	Silt loam	<i>A. campestre, C. monogyna, L.vulgare, P.avium, P. padus, R. cathartica</i>
1-22	22	Gänserndorf	Sandy loam	NA
	13	Gänserndorf	Silt loam	<i>A. campestre, C.mas F. excelsior, J. regia, L. vulgare, P.avium, P. spinus, R. cathartica, R. Canina, V.lantana</i>
	6	Mistelbach	Silt loam	<i>C. betulus, C. monogyna, L.vulgare, P.avium P. domestica, P. spinosa, R. canina</i>
	1	Gänserndorf	Silt loam	<i>J. regia, L. vulgare, P. avium, P. mahaleb</i>

2.3 Particle size SOC fractionation

In this study, a particle size fractionation method was adapted from Spielvogel et al. (2006). The main target of the procedure was to disperse OM from soil aggregates through a two-step ultrasonication treatment with intermediate wet sieving of sonicated samples to different size-fractions which were subsequently measured for OC.

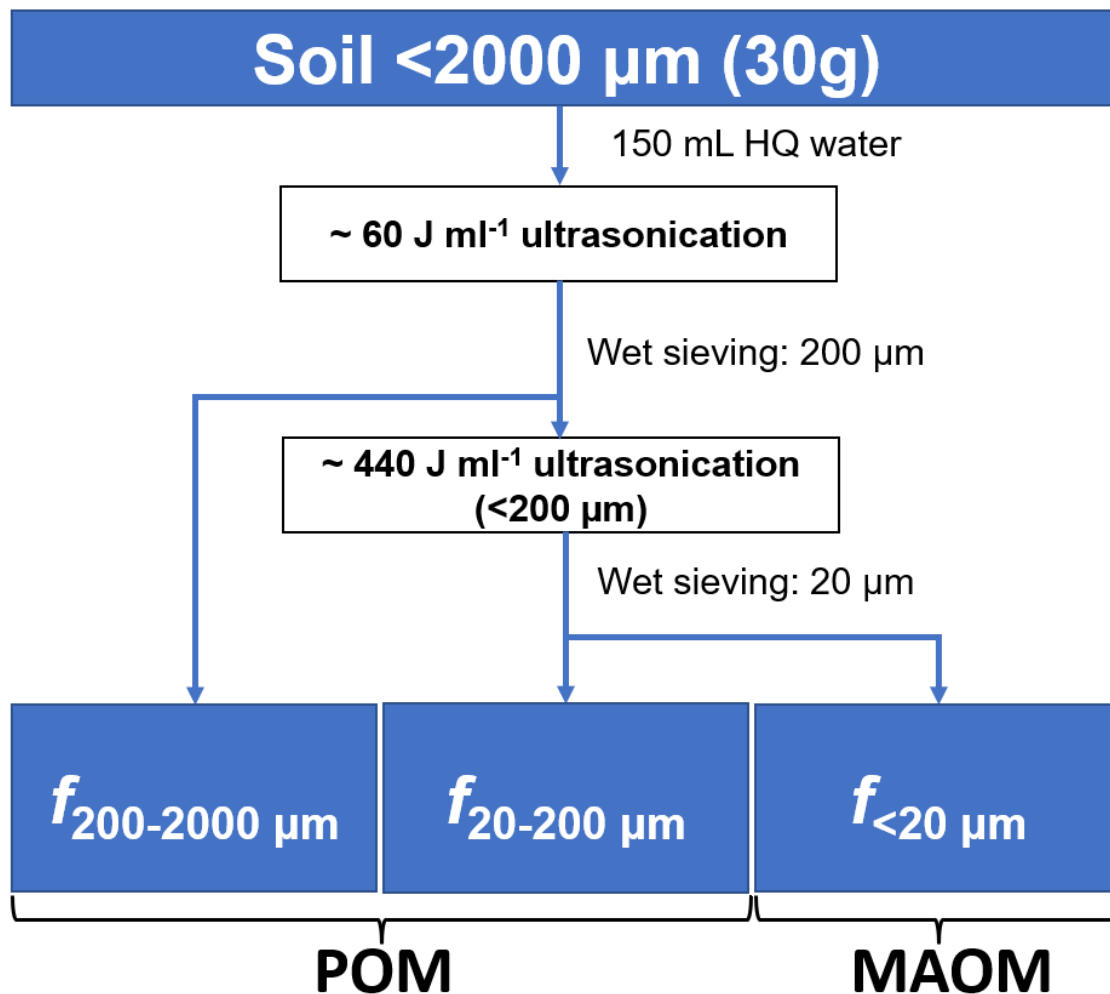


Figure 2.3 Simplified schematic overview of particle size carbon fractionation procedure (own work).

An overview of the particle size fractionation scheme can be seen in Figure 2.3. 150 ml deionized water was added to $2000 \mu\text{m}$ 30 g air-dried soil in a 250 mL sample bottle, obtaining a soil:water ratio of 1:5. Next, the first of two ultrasonic dispersals of the soil-water mixture was performed at 60 J ml^{-1} output energy using a calibrated probe-type sonicator (Sonifier W250-D, Branson Ultrasonics). The probe was submerged 2 cm into the soil-water mixture during the ultrasonication. The first dispersal step was applied to disperse macroaggregates ($>250 \mu\text{m}$) and to then isolate the $f_{>200 \mu\text{m}}$ by wet sieving. Such a preliminary low-intensity ultrasonication was deemed necessary to ensure that large POM particles were not fragmented and redistributed (Amelung and Zech, 1999).

Wet sieving of $f_{>200 \mu\text{m}}$ was then performed using a $200 \mu\text{m}$ mesh sieve which was fixated and shaken for 10 minutes at 50% amplitude in a vibratory sieve shaker system (AS 200, Retsch) into a 1L beaker or cylinder (See Figure 2.4A). During wet sieving, approx. 250 ml of deionized water was pumped through the system via tubing connected to a tap. Upon shaking, the sieve was rinsed with deionized water until the rinsing water was clear. Suspended material ($f_{>200 \mu\text{m}}$) in the beaker was jet pumped into a 2L Schott bottle until as little water as possible remained in the beaker.

The pumped suspension was then sieved again through a $20\text{-}\mu\text{m}$ mesh to ensure light POM and medium silt-sized particles ($f_{200\text{-}20 \mu\text{m}}$) were not falsely added to the $f_{<20 \mu\text{m}}$ MAOM-fraction. The remaining part of the $f_{<20 \mu\text{m}}$ suspension was oven-dried at $105 \text{ }^\circ\text{C}$ to reduce the volume. Deionized water was added to the $f_{<200 \mu\text{m}}$ until volume reached 150 ml and cooled until reaching a temperature $< 5^\circ\text{C}$ before placed in an ice-filled container prior to second ultrasonic dispersal step (see Figure 2.4B). Lowering the suspension temperature was necessary to prevent overheating of the sonicator-probe. Output energy of 440 J ml^{-1} was applied to break down all microaggregates while at the same time avoiding the breakdown of coarse silt-sized SOM-particles (Amelung and Zech, 1999; Yang et al., 2009).

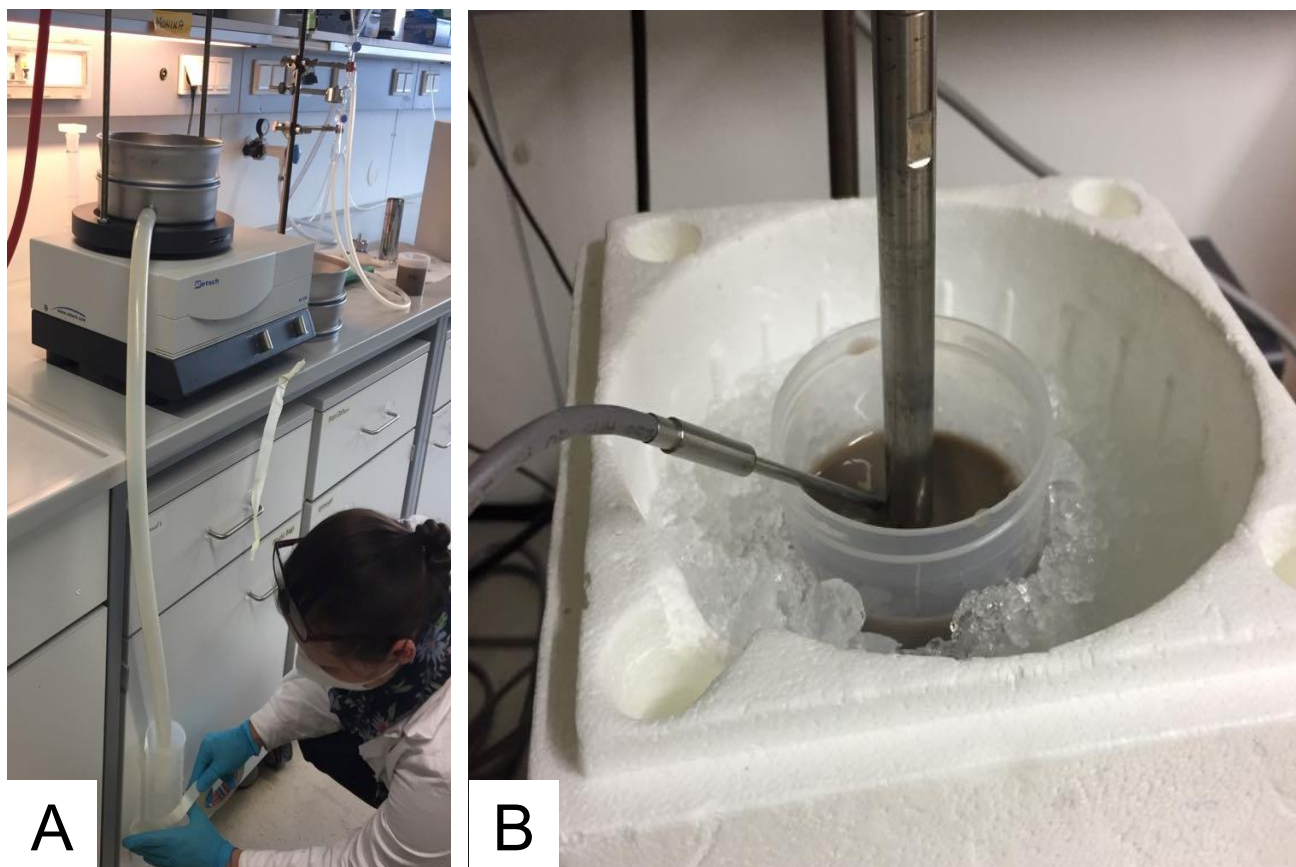


Figure 2.4 Photographs (own) of parts of the fractionation procedure in the lab. A) Set up of wet sieving procedure with water input from tap (red tube in top left corner) and water output into 1L cylinder of the sieve on vibratory sieve shaker system. B) Ultrasonication of sample with ultrasonic probe (from top) and thermometer emerged (on the left).

The now dispersed $f_{<200 \mu\text{m}}$ sample was wet sieved through a $20 \mu\text{m}$ -mesh sieve into the already fractionated $f_{<20 \mu\text{m}}$ from the pumping step, while the $f_{200-20 \mu\text{m}}$ remaining in the sieve was transferred to a porcelain dish. Both fractions were then oven dried at $105 \text{ }^\circ\text{C}$. After drying for at least 24 hours, all fractions were weighed, and $f_{200-20 \mu\text{m}}$ and $f_{<20 \mu\text{m}}$ were homogenized using a pestle, while the $f_{2000-200 \mu\text{m}}$ was milled in a mixer mill for 90 seconds at a frequency of 30 oscillations per second (Retsch MM400). Milling of the large fraction was necessary to achieve satisfactory homogeneity of plant residues.

Total Organic Carbon (TOC) was then determined in a TOC analyzer (Elementar Soli TOC Cube). Between 50-100 mg of sample was weighed in steel crucibles and analyzed in a three-step temperature ramp, thereby yielding TOC at 400°C (TOC400), Residual Organic Carbon (ROC) at 600°C and Total Inorganic Carbon (TIC) at 900°C .

Calibration of sonication probe was continuously performed to ensure correct output energy. 150 ml of deionized water was poured into a sample bottle (without soil) insulated with Styrofoam to minimize heat loss. Next, the “sample” was sonicated at 70 % amplitude (same as used for soil samples), and each minute for 5 minutes the temperature change was recorded for later calculation of the actual energy output. These calculations were used to adjust sonication times to meet the target sonication energies of 60 J ml⁻¹ and 440 J ml⁻¹.

2.4 pH

pH for topsoil was measured in 0.01M CaCl₂ solution. Briefly, 25 mL 0.01M CaCl₂ was added to 10 g of air-dry soil sample. Samples were then shaken and left to equilibrate for 2 hours. After equilibration and soil solids had settled at the bottom, pH was measured in the soil solution using a calibrated pH meter (inoLab pH 730).

2.5 SOC calculations

Measured TOC% (TOC400 + ROC) was initially blank corrected and subsequently SOC concentration [g C kg⁻¹] was calculated for each size fraction on a $f_{<2000 \mu m}$ mass basis (eq.1):

$$(eq.1) \quad SOC_{ci} = \frac{TOC_{\%} \times m_i}{m_{sample}}$$

Where, SOC_{ci} is the SOC [g C kg⁻¹] in fraction *i*, TOC% is the measured TOC in fraction *i* [w/w%], *m_i* is the mass of fraction *i* [g] obtained by particle size fractionation, and *m_{sample}* is mass [kg] of the whole fractionation sample, which was 30g (0.03 kg). SOC in $f_{<2000 \mu m}$ was calculated by summing SOC in all fractions ($f_{2000-200 \mu m} + f_{200-20 \mu m} + f_{<20 \mu m}$).

SOC stocks [t C ha⁻¹] were calculated on both fixed depth (FD) basis and on equivalent soil mass (ESM) basis to account for changes in bulk density (BD) as a function of the hedgerow treatment. Firstly, SOC stocks on a FD basis were calculated for each fraction *i* according to eq.2.

$$(eq.2) \quad SOC_{FDi} = \frac{SOC_{ci} \times BD \times D \times 10^8}{10^6}$$

Where, SOC_{FDi} is the fraction SOC stock [t C ha⁻¹], SOC_{ci} is the fraction SOC concentration as calculated in eq. 1 [w/w%], BD is dry bulk density in $f_{<2000 \mu m}$ [g dry soil cm⁻³], D is the depth of sampling [cm], and 10^8 and 10^6 are conversion factors from cm² to ha and g to t (Mg), respectively.

When assessing temporal changes in SOC stocks as a function of management alterations, the FD approach is not sensitive to soil physical changes represented by BD (Rovira et al., 2015). In other words, when additional litter and root material is added to hedgerow soils or when cultivated soils are tilled, the soil structure and composition is altered, deeming a comparison based on depth alone biased by such changes. An increasingly common approach to avoid such biases is to compare SOC stocks on an ESM basis rather than to a FD. The main idea is to normalize SOC stocks according to a reference soil mass, which is usually set as an initial or control condition (Wendt and Hauser 2013). In this study this will be done by normalizing hedgerow SOC stocks on a cultivated soil mass basis. To estimate ESM SOC stocks, a cumulative coordinate approach (CCA) was used (Juvinyà et al., 2021; Rovira et al., 2015). Firstly, cumulative hedgerow SOC_{FDi} was calculated for the two depth increments (0-20 cm and 20-40 cm) as seen in eq. 2 as well as cumulative fine earth (FE) according to eq. 3.

$$(eq.3) \quad FE_i = m_i \times \left(\frac{m_{sample}}{BD \times D} \right)$$

Where FE_i is the fine earth stock [kg m⁻²], m_i is the mass of fraction i [kg] obtained by particle size fractionation, m_{sample} is mass [kg] of the whole fractionation sample, BD is dry bulk density in $f_{<2000 \mu m}$ [kg dry soil m⁻³], D is the depth of sampling [m].

Then fine mineral earth was calculated by subtracting the OM stock derived from SOC_{FDi} according to eq. 4:

$$(eq.4) \quad FME_i = FE_i - (1.724 \times SOC_{FDi})$$

Where FME_i is fine mineral earth in fraction i [kg m⁻²], FE_i is the fine earth stock [kg m⁻²] as obtained in eq. 3, 1.724 is the Van Bemmelen factor for conversion of OC into OM and SOC_{FDi} is the fraction SOC stock [t C ha⁻¹] as obtained in eq. 2.

Then, cumulative SOC_{FDi} and FME_i were plotted and fitted using a power function ($y = bx^a$, see Figure 2.5).

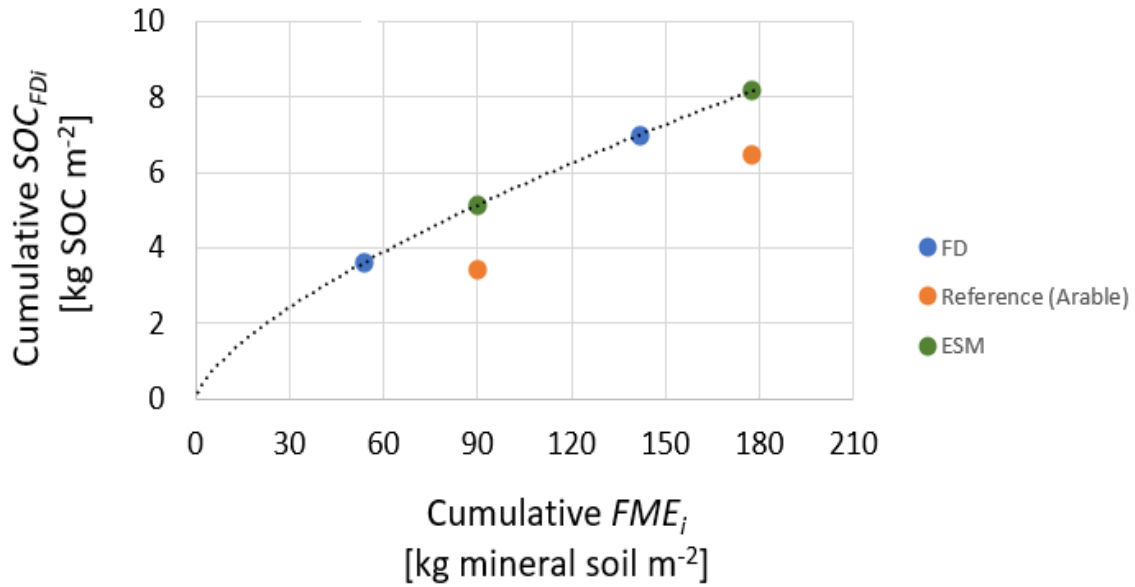


Figure 2.5 Visualization of the cumulative ESM profiles estimated in the study. The example is taken from correcting $f_{<20\mu m}$ SOC stock the 68-year-old hedgerow site in Mistelbach. Using the CCA, hedgerow ESM stocks are represented by green points, obtained by interpolation of the hedgerow FD stocks (blue points) at the cultivated reference cumulative FME (orange points). The power function used for interpolation was derived according to eq. 5.

Parameters were obtained applying least squares (LS) regression which was carried out in MS Excel using the Solver-tool, where fraction specific a and b parameters were estimated by minimizing Sum of Square Errors (SSE). After parameterization, SOC stocks for each depth increment were corrected as according to equation 5, which essentially finds the hedgerow SOC stock corresponding to the cultivated soil mass by solving for y (SOC_{ESM}) using the reference x (FME_R).

$$(eq.5) \quad SOC_{ESM} = b \times FME_R^a$$

Where SOC_{ESM} [kg C m⁻²] is hedgerow SOC stock on FME_R basis, b and a are fitted parameters using LS method. Firstly, the cumulative (0-40 cm) SOC_{ESM} was calculated and converted into t C ha⁻¹ by multiplying with a factor of 10. To calculate SOC_{ESM} for individual depths, FME_R was set to reference 0-20 cm mass to obtain the 0-20 cm corrected hedgerow SOC_{ESM} . Then, the 0-20 cm SOC_{ESM} was subtracted from the cumulative SOC_{ESM} to derive 20-40 cm SOC_{ESM} . Since each fraction in each site has a unique FME_R , SOC stocks will still be referred to according to their depth increment (0-20 cm and 20-

40 cm). It is however important to keep in mind that they are normalized by cultivated soil mass and do not correspond to the actual depth under hedgerows.

SOC sequestration (ΔSOC) [t C ha⁻¹] and SOC sequestration rates [t C ha⁻¹ y⁻¹] were calculated for each fraction according to eq. 6 and eq. 7, respectively.

$$(eq.6) \Delta SOC = SOC_{hedgerow} - SOC_{cultivated}$$

Where ΔSOC is SOC sequestration [t C ha⁻¹], $SOC_{hedgerow}$ is ESM corrected SOC stock under hedgerow [t C ha⁻¹] and $SOC_{cultivated}$ is SOC stock [t C ha⁻¹] under cultivated soil within the same site.

$$(eq.7) SOC \text{ sequestration rate} = \frac{\Delta SOC}{\Delta t}$$

Where SOC sequestration rate [t C ha⁻¹ y⁻¹] is the ΔSOC relative to the difference in chronosequence timespan Δt [years] of interest. Δt was thus both represented as average age of hedgerow age group and for the whole chronosequence.

2.6 C_{sat} and C_{def}

C_{sat} and C_{def} were calculated based on the eq. 8 derived by Wenzel et al. (2022) based boundary line (BL) regression of the 90th percentile of SOC concentrations [g C kg⁻¹] in $f_{<20 \mu m}$ of grassland soils in Lower Austria.

$$(eq.8) C_{sat} = 1.227 (\pm 0.0625) \times mineral f_{<20 \mu m}$$

Where C_{sat} is the carbon saturation potential [g C kg⁻¹], 1.227 (± 0.0625) is the slope obtained for the BL parameterization and $mineral f_{<20 \mu m}$ is the proportion of mineral soil <20 μm [% of <2000 μm]. The proportion of $mineral f_{<20 \mu m}$ was in this study derived by subtracting the mass of OM (defined as 1.724 multiplied by OC) from the recovered mass of $f_{<20 \mu m}$ in the fractionation procedure. C saturation deficit, C_{def} , was subsequently calculated by subtracting the current SOC concentration in $f_{<20 \mu m}$ from C_{sat} .

C_{sat} and C_{def} values were also calculated as stocks [t C ha⁻¹] using the FD approach as described in eq. 2 assuming the same BD as for $f_{<2000 \mu m}$.

2.7 Statistical analyses

Statistical analyses were conducted with R version 4.03 (R Core Team, 2020) in RStudio version 1.3.1093 (RStudio Team, 2020). Prior to statistical testing, data was assessed for parametric test assumptions, namely normality, and homogeneity of variance. If assumptions were not met, data was log-transformed and if such a transformation was successful in respect to parametric assumptions, means and error terms were reported for untransformed data. When two groups of means were compared, Shapiro-Wilk's Test of Normality and Levene's Test for Homogeneity of Variance were used to assess assumptions for using Student's T-test. When compared groups did not meet assumptions, Wilcoxon Rank Sum Test was applied. When a mean was tested for significance from 0, one-sample t-tests or one-sample Wilcoxon Rank Sum Tests were used. When a dependent variable was modelled with explanatory variables of multiple levels or when performing linear regression analyses, linear model residual plots and Normal Quantile-Quantile plots were visually inspected to assess homoscedasticity and normality, respectively. If assumptions were met, Analysis of Variance (ANOVA) was applied with Tukey HSD posthoc test to compare individual differences among groups. When assumptions were not fulfilled, non-parametric Kruskal Wallis Rank Sum Test and Pairwise Wilcoxon Rank Sum Test with Bonferroni corrections to compare individual differences among groups were used. All tests were carried out at the $p = 0.05$ significance level. Graphs were created in GraphPad Prim 8.0.2 and tables in MS Excel and MS Word version 2204.

3. Results

In the following section results will be presented in figures or tables and will include the results of statistical analyses.

3.1 Basic soil properties

Summarized basic soil properties grouped by land use and depth are presented in Table 3.1 and photographs of selected sites can be seen in Figure 3.1. BD was significantly lower in 0-20 cm layer compared to 20-40 cm, in both arable ($p = 0.03$) and hedgerow soils ($p > 0.001$). Furthermore, hedgerow soil BD in 0-20 cm layer was significantly lower than in cultivated soils of the same depth ($p > 0.001$),

Table 3.1 Average bulk density (BD) [g cm^{-3}], organic matter (OM) [g kg^{-1}], inorganic carbon (IC) [g kg^{-1}] and pH [0.01M CaCl_2] values by land use and soil depth increment [cm]. Figures are reported in \bar{x} (SE). Raised letters indicate statistical significance at the $p < 0.05$ significance-level, where uppercase letters indicate depth differences between same fractions and same land use (paired t-test), while lowercase letters indicate land use differences between same depth increments (two sample t-test).

<i>Land use</i>	<i>Depth</i> [cm]	<i>No. of samples</i>	<i>Bulk density</i> [g cm^{-3}]	<i>OM</i> [g kg^{-1}]	<i>IC</i> [g kg^{-1}]	<i>pH</i> [0.01M CaCl_2]	<i>Mineral particles</i> $f_{<20\mu\text{m}}$ [%]
Arable	0-20	13	1.33 (0.04) ^{Aa}	31.5 (2.0)	9.5 (2.5) ^{Aa}	7.42 (0.02) ^a	50.4 (2.9) ^a
	20-40	13	1.48 (0.05) ^{Ba}	27.2 (3.2)	13.1 (3.0) ^{Aa}	–	49.7 (2.7) ^a
Hedge	0-20	13	1.08 (0.05) ^{Ab}	46.4 (3.3)	9.4 (2.7) ^{Aa}	7.28 (0.04) ^b	48.3 (2.5) ^a
	20-40	13	1.35 (0.04) ^{Ba}	30.1 (2.5)	9.4 (2.8) ^{Aa}	–	49.5 (2.7) ^a

while not significantly lower in the 20-40 cm layer ($p = 0.051$). BD and SOC concentrations were significantly negatively correlated in both depth increments (Figure 3.2) Thus, as SOC increases under hedgerows, BD systematically decreased, creating a bias in SOC stock estimations based on BD. With this observation, SOC stocks will from now on be reported in ESM rather than FD.

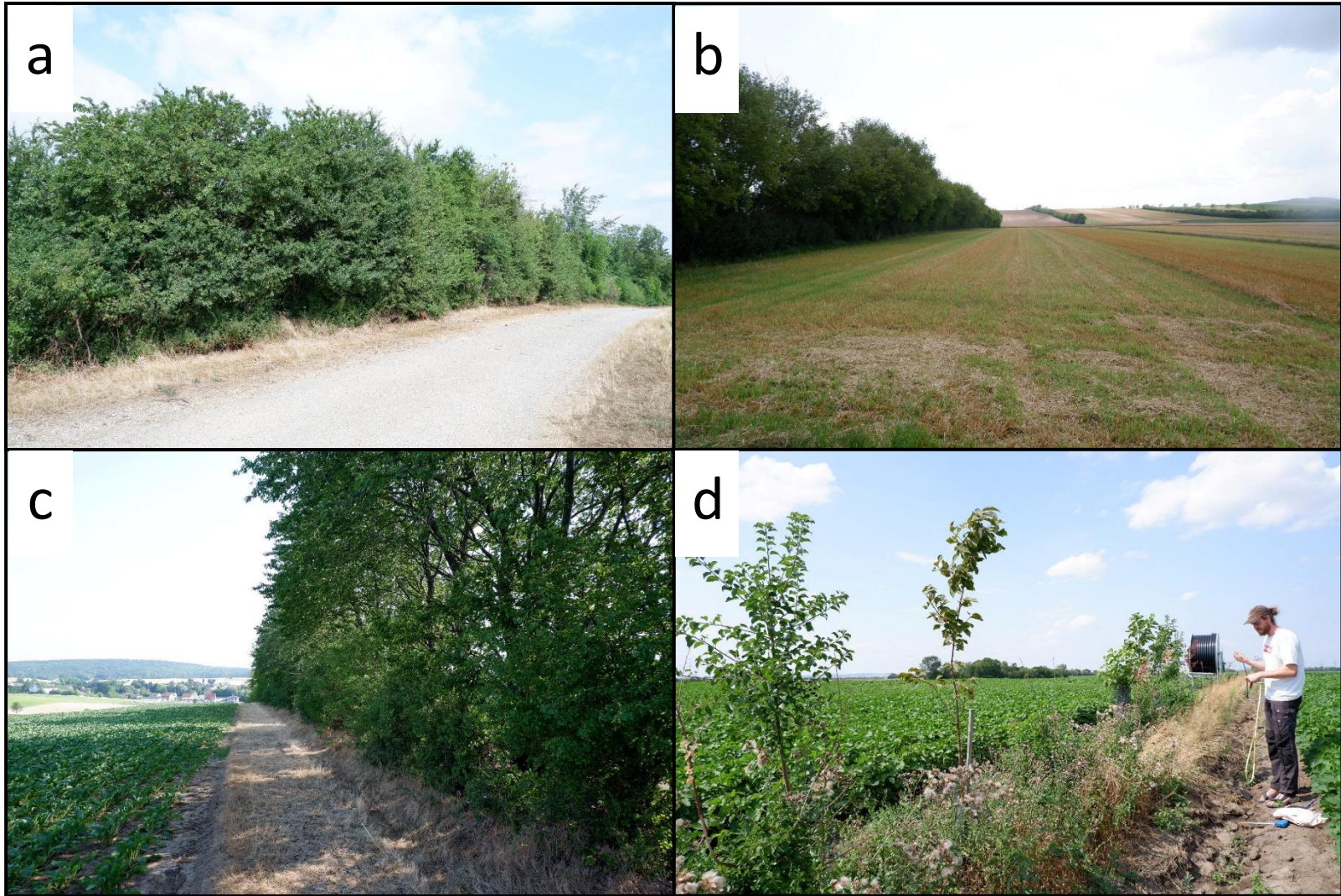


Figure 3.1 Four selected hedgerow-field sites: a) Schrick, Mistelbach district , hedgerows planted 1950 b) Diepolz, Mistelbach district, hedgerows planted 1970 c) Oberkreuzstetten, Mistelbach district, hedgerows planted 2014 d) Aderklaa, Gänserndorf district, hedgerows planted 2019.

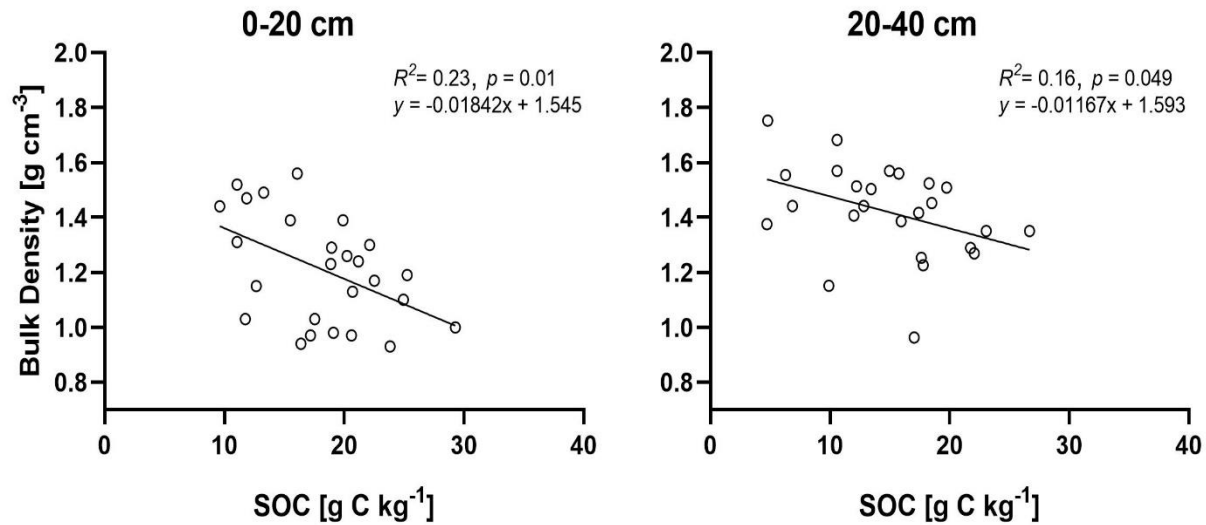


Figure 3.2 Linear relationship between bulk density [g cm^{-3}] and SOC [g C kg^{-1}] in the 0-20 and 20-40 cm depth. Coefficients of determination, p-values (at the 0.05 significance level) for a non-zero slope and modelled linear equations are reported.

OM was calculated based on SOC ($1.724 * f_{<2000 \mu\text{m}} \text{SOC}$) which will later be elaborated. Inorganic carbon (IC) did not seem to be affected by hedgerows. pH was only measured for topsoil and was found to be slightly lower in hedgerow soils (Table 3.1, $p = 0.02$). Mineral particles $f_{<20 \mu\text{m}} [\%]$ varied insignificantly between land use.

3.2 SOC stock calculation methods

Corrected estimates of hedgerow SOC stocks on an ESM basis resulted in relative changes ranging from -7% to 28% (mean = 14%) and -11% to 31% (mean = 7%) in 0-20 cm and 20-40 cm, respectively compared to FD (Figure 3.3). In the 0-20 cm layer, ESM values were significantly larger than FD ($p < 0.01$), while differences in methods were not significant in the 20-40 cm layer (Figure 3.3). FD and ESM SOC estimates were also evaluated across hedge age group and particle size fractions to explore how the ESM recalculation affected SOC across the groups of interest – these data are presented in Appendix A. SOC calculation method did not significantly affect $f_{<2000 \mu\text{m}} \text{SOC}$ across age groups, however

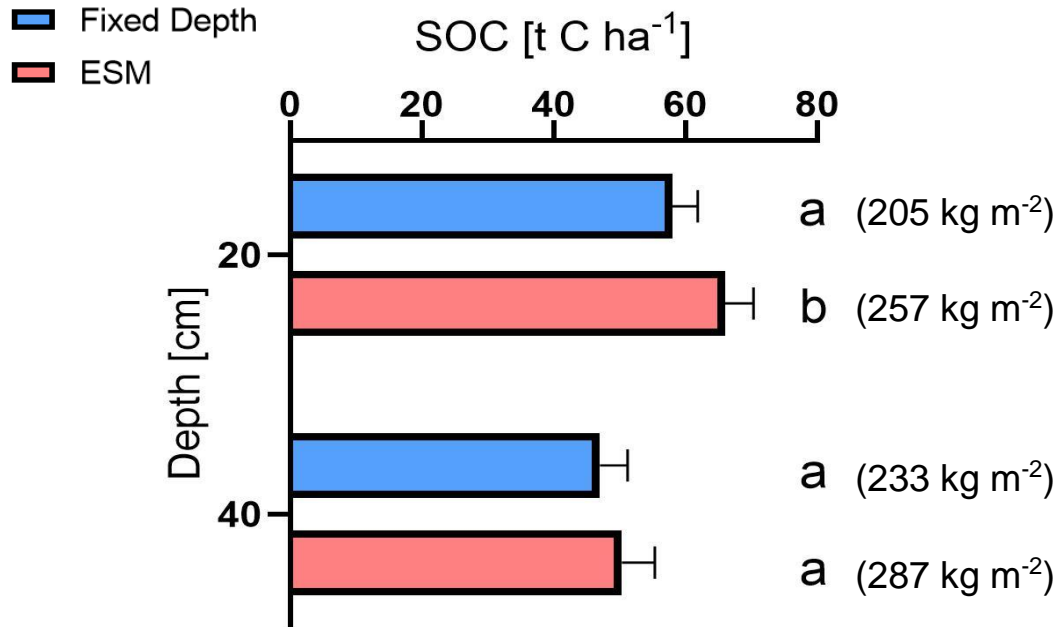


Figure 3.3 Hedgerow SOC stocks [t C ha⁻¹] by SOC estimation method (ESM and fixed depth) and depth increment (0-20 and 20-40 cm). Values are reported in means with standard error (SE) bars. Lower case letters indicate statistical significance at the $p < 0.05$ significance-level tested using paired t-tests. Mean hedgerow and reference FME [kg mineral soil m⁻²] for both depth increments are reported next to bar charts. SOC calculated on ESM basis uses reference FME.

in topsoil, FD underestimations of SOC tended to be more pronounced in older hedge age groups (30-45- and 50-70-year groups) compared to the 1-22-year group. Such tendencies were less evident in the subsoil. Among fractions, significant effects of SOC calculation were found in the 0-20 cm layer where $f_{2000-200 \mu m}$ was significantly ($p < 0.01$) higher in FD compared to ESM (median increase of 25%). The opposite trend was evident in the finer fractions, as ESM estimated higher SOC values in the $f_{200-20 \mu m}$ (median increase of 10%) and $f_{<20 \mu m}$ (mean increase of 16%). In the 20-40 cm layer no significant differences were found, however FD tended to underestimate SOC in all fractions compared to ESM.

3.3 SOC stocks in bulk soil (< 2000 μm)

Average SOC stocks under hedgerows and cultivated fields across the entire chronosequence are shown in Figure 3.4. Hedgerow $f_{<2000\ \mu\text{m}}$ SOC stocks were on average $66.0\ \text{t C ha}^{-1} \pm 4.3$ in the 0-20 cm layer compared to arable SOC stocks of $47.9\ \text{t C ha}^{-1} \pm 2.8$. This difference was significant ($p < 0.01$) and equivalent to a 38% stock increase. SOC concentrations were also significantly different ($p < 0.01$) with averages of ($26.9\ \text{g C kg}^{-1} \pm 1.9$) under hedgerows and ($18.2\ \text{g C kg}^{-1} \pm 1.2$) arable fields – equal to an increase of 48%.

In the 20-40 cm layer differences were less apparent. Subsoil SOC stocks were on average $50.4\ \text{t C ha}^{-1} \pm 5.0$ under hedgerows and $45.8\ \text{t C ha}^{-1} \pm 4.8$ under arable fields. While hedgerow stocks were slightly higher in the 20-40 cm layer on average, means did not differ significantly ($p = 0.52$). Differences in average SOC concentration were relatively larger than stocks in the 20-40 cm layer, but still not to a significant degree ($p = 0.18$). Furthermore, the 0-20 cm of hedgerow soils stored 31% larger stocks than the 20-40 cm ($p = 0.02$), while SOC stocks in arable soil were not significantly different between the two depth increments ($p = 0.46$). When SOC concentrations were considered, depth differences were evident

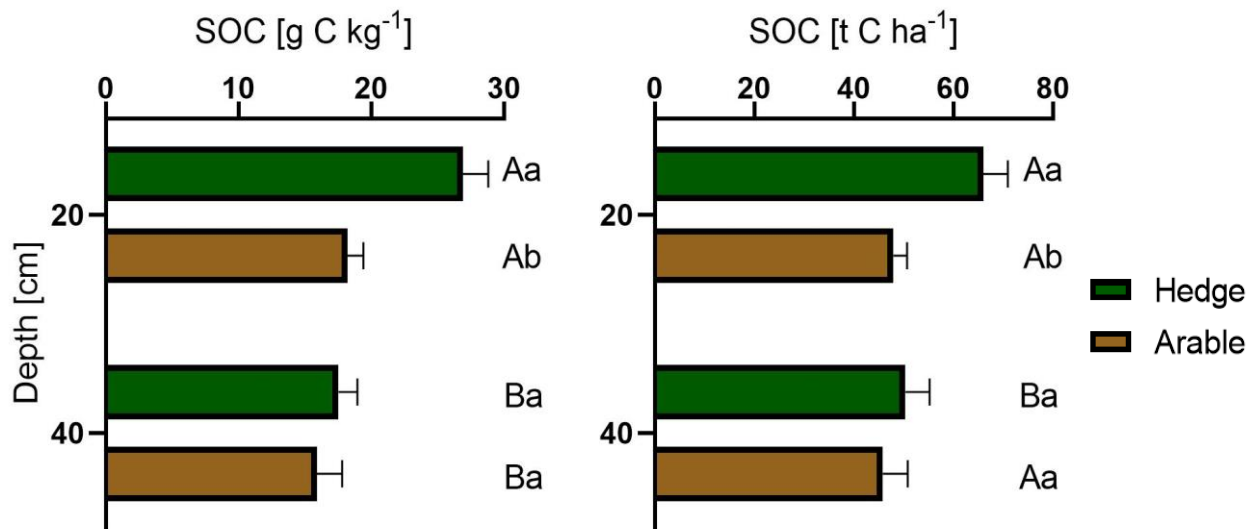


Figure 3.4 Mean (SE bars) $f_{<2000\ \mu\text{m}}$ SOC stock [t C ha⁻¹] and SOC concentrations [g C kg⁻¹] by land use in two depth increments (0-20 and 20-40 cm). Uppercase letters indicate depth differences between same fractions and same land use (paired t-test), while lowercase letters indicate land use differences between same depth increments (unpaired t-test).

under both hedgerow ($p = 0.002$) and arable fields ($p = 0.008$), equivalent to relative decreases from topsoil to subsoil of 54% and 15%, respectively.

Considering the whole studied soil profile (0-40 cm), hedgerows did not significantly accumulate SOC stocks above the cultivated baseline ($p = 0.06$). The marginally insignificant result is reflected in mean hedgerow stocks of $115 \text{ t C ha}^{-1} \pm 7.5$, markedly higher than the $93.8 \text{ t C ha}^{-1} \pm 7.3$ found in the top 40 cm of cultivated soil. When SOC concentrations were compared, this difference was significant ($p = 0.04$) and equal to an increase of 9.05 g C kg^{-1} (21%).

3.4 SOC in particle size fractions

Partitioning of SOC into particle size fractions on a $<2000 \mu\text{m}$ soil basis across depth and management is shown in Figure 3.5. SOC was distributed unevenly across fractions, the majority being stored in the $f_{<20 \mu\text{m}}$ fraction, the remainder hereof predominately present in the $f_{200-20 \mu\text{m}}$ fraction, leaving the $f_{2000-200 \mu\text{m}}$

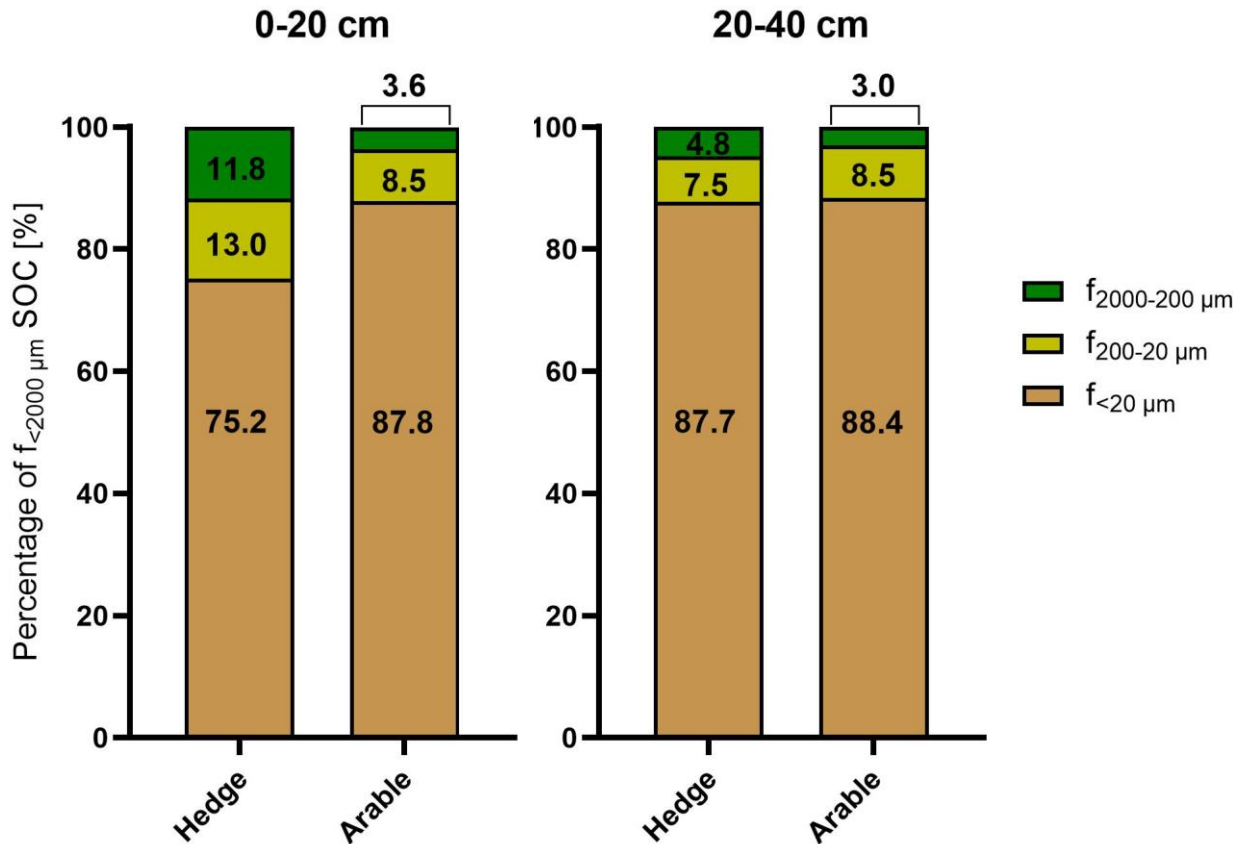


Figure 3.5 Mean relative distribution [%] of $f_{<2000 \mu\text{m}}$ SOC stock [t C ha⁻¹] by SOC particle size fraction and land use in two depth increments (0-20 and 20-40 cm).

μm fraction as the smallest pool. Furthermore, distributions of SOC in particle size fractions differed across management and depth. In the 0-20 cm layer, hedgerow soils contained relatively more SOC within POM fractions than soils under cultivation (Figure 3.5). Consequently, a lesser percentage of hedgerow SOC ($75.2\% \pm 2.5$) was stored in $f_{<20 \mu\text{m}}$ compared to arable soils ($87.8\% \pm 1.3$). Hedgerow planting seemed to have a negligible effect on the relative SOC fraction distribution in the 20-40 cm layer.

Topsoil SOC sequestration in bulk soil provided by hedgerows was reflected in SOC stocks of particle size fraction (Table 3.2). In $f_{2000-200 \mu\text{m}}$, both hedgerow SOC stocks and concentrations were significantly larger ($p < 0.001$) than arable. Differences in the topsoil $f_{2000-200 \mu\text{m}}$ SOC was equal to median increases of 3.9 t C ha^{-1} (315%) and 2.5 g C kg^{-1} (466%). In $f_{200-20 \mu\text{m}}$ differences were also significant ($p < 0.001$) and equal to median increases of 3.4 t C ha^{-1} (89%) and 1.7 g C kg^{-1} (126%). In the $f_{<20 \mu\text{m}}$ fraction, SOC stocks under hedgerows across the entire chronosequence did not differ significantly from arable stocks ($p = 0.053$), while when concentrations were considered, differences were significant ($p < 0.01$), equivalent to mean increases of 3.9 g C kg^{-1} (24%). No significant differences in individual fraction SOC stocks or concentrations were found between hedgerow and soils in the 20-40 cm layer (Table 3.2).

Depth distribution of particle size fractions differed within each land use. In hedgerow soils, depth differences were significant in the $f_{2000-200 \mu\text{m}}$ ($p < 0.01$), $f_{200-20 \mu\text{m}}$ ($p < 0.001$) and $f_{<20 \mu\text{m}}$ ($p < 0.001$), while no such significant differences were found in arable soils. SOC concentrations were however significantly higher in arable topsoil than subsoil in the $f_{200-20 \mu\text{m}}$ ($p = 0.03$) and $f_{<20 \mu\text{m}}$ ($p = 0.008$), equivalent to relative decreases with depth of 21% and 12%.

Table 3.2 SOC in particle size fractions for hedgerow and arable soils in two depth increments (0-20, 20-40 cm). SOC values are both given in stocks [t C ha⁻¹] concentrations [g C kg⁻¹] and reported in mean with standard error (SE) and median with interquartile range (IQR). Both measures of central tendency are given as not all groups were normally distributed. Raised letters indicate statistical significance at the $p < 0.05$ significance-level, where uppercase letters indicate depth differences between same fractions and same land use (paired t-test or Wilcoxon rank-sum test), while lowercase letters indicate land use differences between same fractions and same depth (unpaired t-test or Wilcoxon rank-sum test).

Land use	Depth [cm]	Particle size fraction	SOC			
			t C ha ⁻¹		g C kg ⁻¹	
			Mean (SE)	Median (IQR)	Mean (SE)	Median (IQR)
Arable	0-20	$f_{2000-200 \mu m}$	1.59 (0.28)	1.22 (1.47) ^{Aa}	0.59 (0.01)	0.54 (0.54) ^{Aa}
		$f_{200-20 \mu m}$	3.95 (0.28)	3.77 (1.52) ^{Aa}	1.50 (0.10)	1.32 (0.53) ^{Aa}
		$f_{<20 \mu m}$	42.39 (2.86) ^{Aa}	46.54 (16.70)	16.20 (1.23) ^{Aa}	16.38 (8.0)
	20-40	$f_{2000-200 \mu m}$	1.12 (0.26)	0.85 (0.60) ^{Aa}	0.46 (0.11)	0.31 (0.30) ^{Aa}
		$f_{200-20 \mu m}$	3.23 (0.24)	3.27 (0.80) ^{Aa}	1.20 (0.10)	1.04 (0.45) ^{Ba}
		$f_{<20 \mu m}$	39.54 (4.71) ^{Aa}	41.98 (21.11)	14.20 (1.80) ^{Ba}	15.75 (7.69)
Hedgerow	0-20	$f_{2000-200 \mu m}$	5.84 (0.87)	5.07 (2.68) ^{Ab}	3.21 (0.48)	3.06 (1.94) ^{Ab}
		$f_{200-20 \mu m}$	8.38 (1.01)	7.14 (5.07) ^{Ab}	3.61 (0.51)	2.98 (3.14) ^{Ab}
		$f_{<20 \mu m}$	51.78 (3.6) ^{Aa}	55.68 (19.6)	20.11 (1.43) ^{Ab}	20.61 (6.64)
	20-40	$f_{2000-200 \mu m}$	2.46 (0.63)	2.09 (2.30) ^{Ba}	0.74 (0.10)	0.84 (0.41) ^{Ba}
		$f_{200-20 \mu m}$	3.65 (0.40)	3.50 (1.08) ^{Ba}	1.25 (0.81)	1.25 (0.21) ^{Ba}
		$f_{<20 \mu m}$	44.26 (4.88) ^{Ba}	43.08 (14.73)	15.46 (1.43) ^{Ba}	14.98 (5.42)

Linear regressions between particle size SOC fractions were calculated in the 0-20 cm layer, as this was the layer where significant variations occurred among experimental units (Figure 3.6). This was done to elucidate relationships explaining sequential breakdown of SOM in a descending order of particle size: $f_{2000-200\ \mu\text{m}}$ (coarse POM) \rightarrow $f_{200-20\ \mu\text{m}}$ (medium-sized POM) \rightarrow $f_{<20\ \mu\text{m}}$ (fine POM and MAOM). No

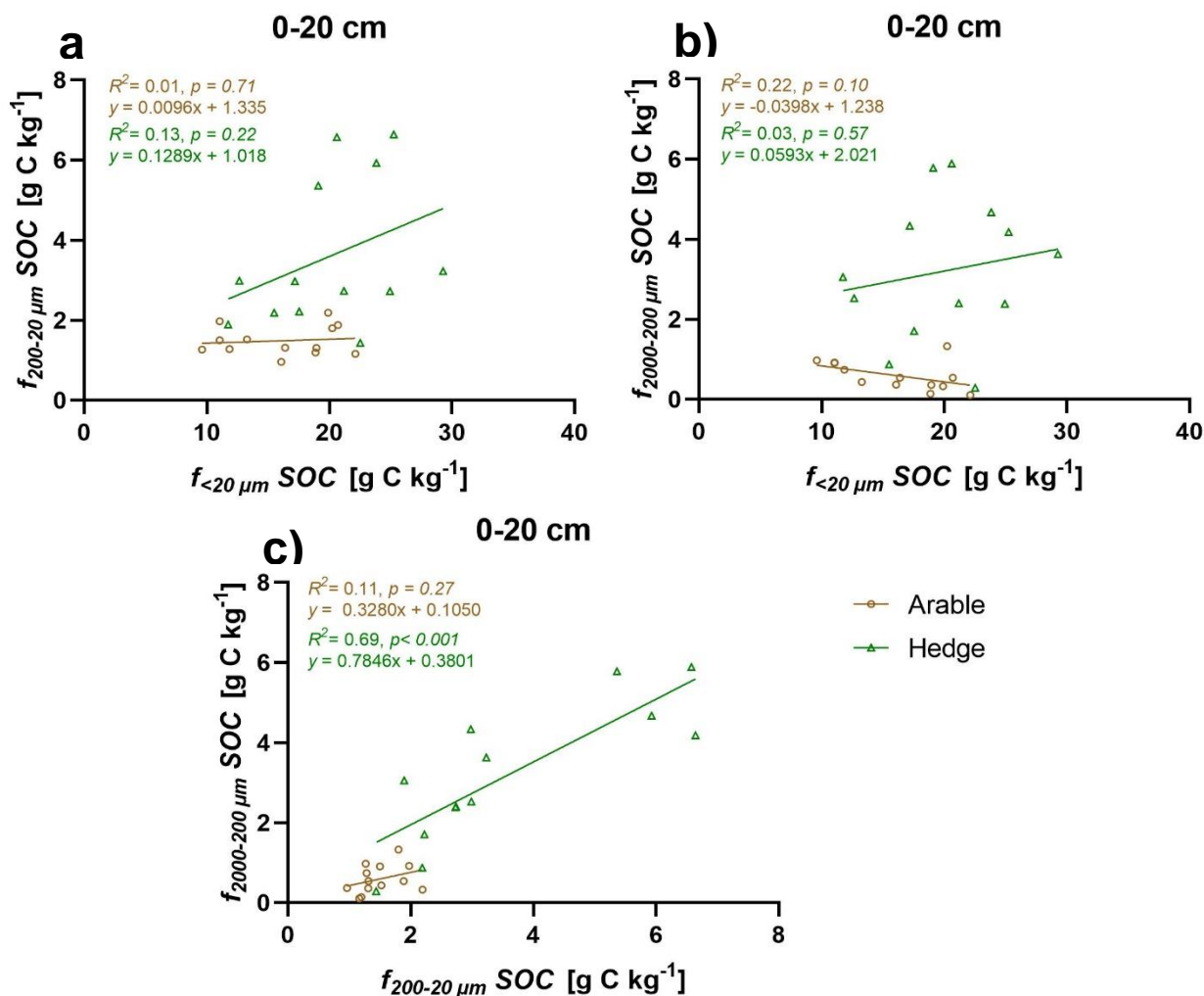


Figure 3.6 Linear relationships between particle size SOC fractions in the 0-20 cm soil layer for both hedgerow and arable soils: a) between SOC in $f_{200-20\ \mu\text{m}}$ and $f_{<20\ \mu\text{m}}$ b) between SOC in $f_{2000-200\ \mu\text{m}}$ and $f_{<20\ \mu\text{m}}$ c) between SOC in $f_{2000-200\ \mu\text{m}}$ and $f_{200-20\ \mu\text{m}}$. Coefficients of determination, p-values (at the 0.05 significance level) for a non-zero slope, and modelled linear equations are reported for each land use

significant relationships were found between SOC in $f_{<20\ \mu\text{m}}$ and SOC in $f_{200-20\ \mu\text{m}}$ and $f_{2000-200\ \mu\text{m}}$ (Figure 3.6a and 3.6b). However, a moderate relationship was found between $f_{200-20\ \mu\text{m}}$ and $f_{2000-200\ \mu\text{m}}$, where SOC in $f_{2000-200\ \mu\text{m}}$ could explain 69% of the variance in $f_{200-20\ \mu\text{m}}$ SOC (Figure 3.6c).

3.5 SOC sequestration over time

To evaluate the SOC sequestration of hedgerows in the chronosequence, absolute differences between hedgerow and cultivated SOC stocks (Δ SOC) were calculated across depth and particle size fraction. Subsequently, age dependency of Δ SOC was analyzed through linear regression (Table 3.3) and by comparing Δ SOC of hedgerow age groups (Figure 3.8). Linear regression analyses revealed that only the $f_{2000-200 \mu m}$ in the 0-20 cm layer could be significantly predicted by hedgerow age, explaining 42% of Δ SOC (Figure 3.7). Δ SOC in $f_{<2000 \mu m}$ and $f_{200-20 \mu m}$ showed age trends as p-values for slopes were between 0.07 and 0.08. Topsoil $f_{<20 \mu m}$ SOC and all fractions in subsoil were not linearly correlated with hedgerow age (Table 3.3). On a 0-40 cm depth basis, a linear trend was observed in the $f_{2000-200 \mu m}$. Graphical representation linear regressions in subsoil are shown in Appendix B.

Age group comparisons of Δ SOC showed similar results. While ANOVA and Kruskal-Wallis tests revealed no significant differences in Δ SOC among age groups (Figure 3.8), topsoil $f_{2000-200 \mu m}$ showed a trend ($p=0.054$). Accordingly, post-hoc tests revealed that the oldest hedgerows (50-70 years) sequestered significantly more SOC than the youngest (1-22 years). In the 0-40 cm, Δ SOC in $f_{2000-200 \mu m}$ and $f_{200-20 \mu m}$ followed the trend in 0-20 cm (but no significant differences), while means in the $f_{<20 \mu m}$ and $f_{<2000 \mu m}$ exhibited high variation. A supplementary graph of Δ SOC among age groups in 20-40 cm can be found in Appendix C.

SOC sequestration entails that hedgerows accumulate SOC stocks above the level of soils under cultivation within a given timeframe. Therefore, if mean or median Δ SOC of a site age group were significantly higher than 0, this may be interpreted as sequestration. Consequently, Δ SOC in each age group was tested for significant differences from 0 (Table 3.4). In topsoil, significant positive Δ SOC in $f_{<2000 \mu m}$ and $f_{<20 \mu m}$ could be found for the oldest hedgerows ($p = 0.01$) and ($p = 0.009$), respectively, equal to sequestration rates of ($0.39 \text{ t C ha}^{-1} \text{ y}^{-1}$) and ($0.18 \text{ t C ha}^{-1} \text{ y}^{-1}$), respectively (Table 3.4). Δ SOC in the two younger hedgerow age groups did not significantly sequester SOC (Δ SOC not different from 0), however p-values indicated trends ($p < 0.08$ in the 30–45-year groups) in $f_{2000-200 \mu m}$ and $f_{<20 \mu m}$. All sequestration values tested for significance from 0 are shown in Appendix D.

Δ SOC in $f_{2000-200 \mu m}$ and $f_{200-20 \mu m}$ were not significantly higher than 0, which may have been due to the employed non-parametric tests with less statistical power, reflecting the high heteroscedasticity among age groups in these fractions. However, drawing on the significantly higher SOC stocks in $f_{<2000 \mu m}$, f_{2000-}

200 μm , and $f_{200-20 \mu\text{m}}$ under hedgerows, compared to cultivated soils for the whole chronosequence (1-70 years), ΔSOC and associated sequestration rates were estimated. This approach yielded sequestration rates of (0.48 t C ha⁻¹ y⁻¹) in $f_{<2000 \mu\text{m}}$, thus leading to sequestration rates ranging from (0.39 – 0.48 t C ha⁻¹ y⁻¹) depending on whether only old hedgerows or the entire chronosequence (1-70 years) is considered. Furthermore, sequestration rates of (0.1 t C ha⁻¹ y⁻¹) and (0.09 t C ha⁻¹ y⁻¹) were estimated in $f_{2000-200 \mu\text{m}}$ and $f_{200-20 \mu\text{m}}$ over the entire chronosequence, which is close to the slopes estimated through linear regression (Table 3.3).

Table 3.3 Results of linear regression analyses of differences between hedgerow and arable SOC stocks in each sample site (ΔSOC [t C ha⁻¹]) as a function of hedgerow age [years] across particle size fractions and depth increments. Best-fit values with significant ($p>0.05$) and marginally insignificant ($p>0.1$) non-zero slopes are marked in bold and assigned (*) and (.), respectively.

Depth [cm]	Fraction [μm]	SOC [t C ha ⁻¹]			
		Slope	Intercept	R ²	P-value
0-20	$f_{<2000 \mu\text{m}}$	0.24	9.30	0.27	0.07 .
	$f_{2000-200 \mu\text{m}}$	0.09	0.96	0.42	0.02 *
	$f_{200-20 \mu\text{m}}$	0.09	1.14	0.24	0.08 .
	$f_{<20 \mu\text{m}}$	0.06	7.22	0.06	0.42
20-40	$f_{<2000 \mu\text{m}}$	-0.15	12.23	0.05	0.47
	$f_{2000-200 \mu\text{m}}$	0.01	1.02	0.02	0.65
	$f_{200-20 \mu\text{m}}$	-0.00	0.55	0.00	0.87
	$f_{<20 \mu\text{m}}$	-0.16	10.65	0.06	0.45
0-40	$f_{<2000 \mu\text{m}}$	0.05	21.85	0.01	0.80
	$f_{2000-200 \mu\text{m}}$	0.09	2.01	0.29	0.07 .
	$f_{200-20 \mu\text{m}}$	0.06	2.01	0.14	0.22
	$f_{<20 \mu\text{m}}$	-0.13	18.40	0.04	0.53

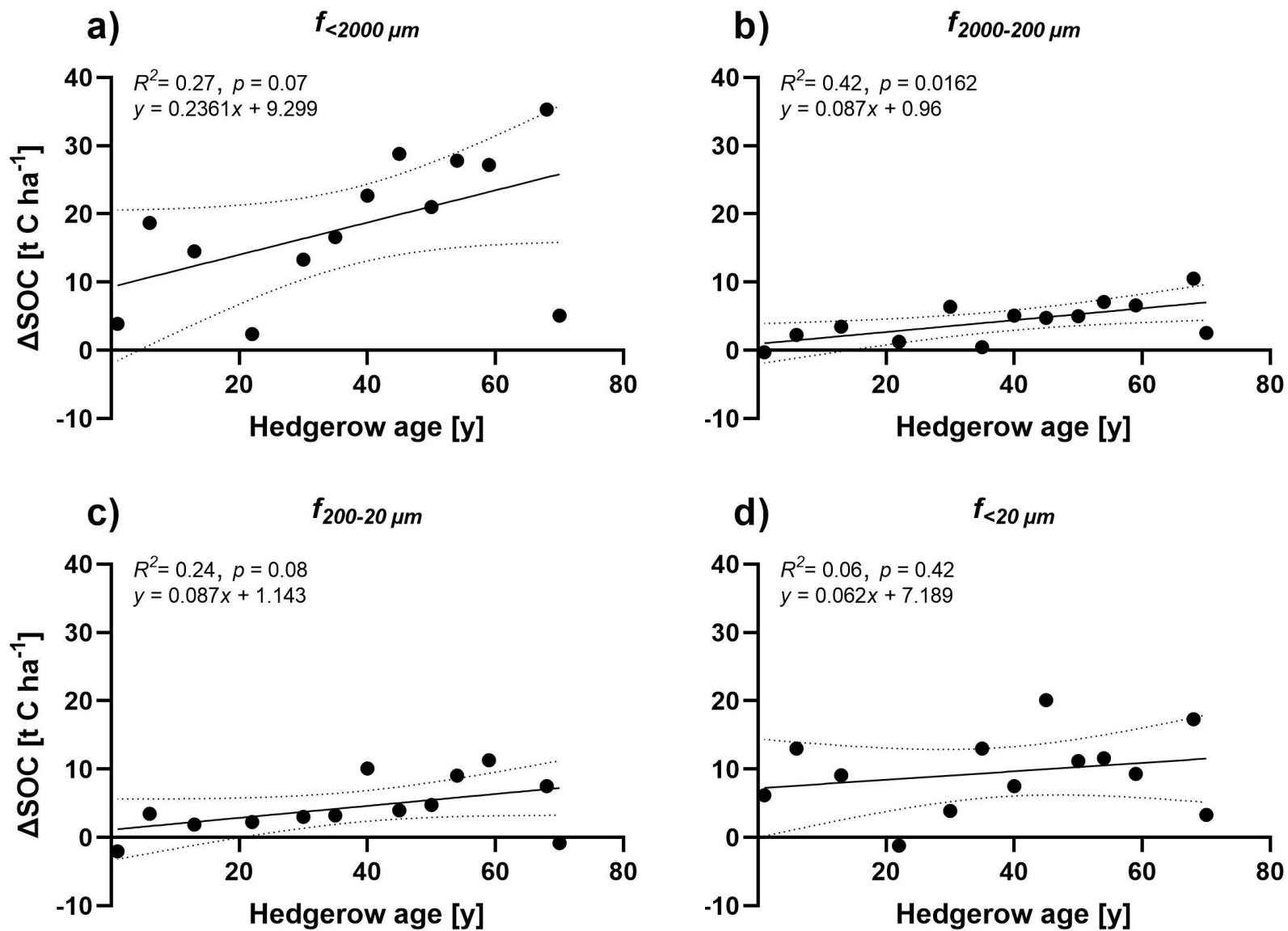


Figure 3.7 Linear regressions of differences between hedgerow and arable SOC stocks in each sample site (ΔSOC [t C ha^{-1}]) as a function of hedgerow age [years] for four particle size fractions in the 0-20 cm layer: a) $f_{<2000}$ b) $f_{2000-200 \mu\text{m}}$ c) f_{200-20} d) $f_{<20 \mu\text{m}}$. Solid lines represent best-fit lines and dotted lines show its 95% confidence intervals. R^2 , p -values and regression equations are reported.

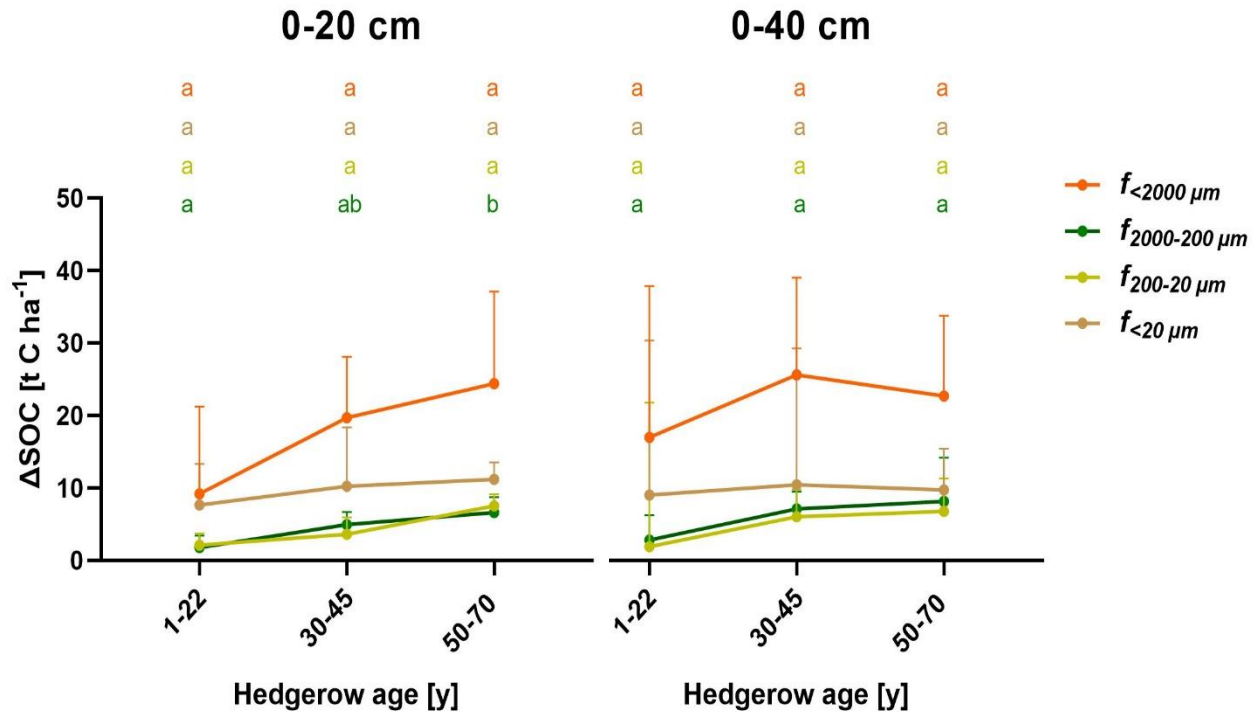


Figure 3.8. SOC sequestration (Δ SOC, t C ha⁻¹) by hedgerow age groups in 0-20 cm and 0-40 cm soil layers. Points are reported in medians with IQR error lines. Lower case letters display statistical significance at the p<0.05 significance level informed by Tukey HSD and Pairwise Wilcoxon Signed Rank Sum post-hoc tests following ANOVA and Kruskal Wallis Rank Sum Test, respectively.

In the 20-40 cm layer, Δ SOC were not significantly different from 0 across fractions and age groups, confirming previous results of limited subsoil changes. While hedgerow SOC stocks were not significantly larger than in arable soil down to 40 cm when averaged over the chronosequence, the age groups allowed for some additional trends to be observed. In $f_{<2000 \mu m}$, $f_{2000-200 \mu m}$ and $f_{200-20 \mu m}$ Δ SOC was found to be significantly different from 0 in older hedgerows (Table 3.4). In $f_{<2000 \mu m}$, $f_{2000-200 \mu m}$ significant sequestration was observed in the 50–70-year group, while Δ SOC in $f_{200-20 \mu m}$ were only significant in the 30-45-year group and not in the oldest and youngest age classes.

Table 3.4 SOC sequestration [Δ SOC in $t\ C\ ha^{-1}$] and SOC sequestration rates [$t\ C\ ha^{-1}y^{-1}$] by SOC fraction and hedgerow age groups found to be significantly different from 0. Δt is the average year of the age group used to calculate sequestration rates. Group sequestration values were tested at $p < 0.05$ significance level using one-sample t-tests and for 1–70-year group according to significant differences tested using two-sample t-tests between hedgerows and cultivated soils in each depth increment.

<i>Depth</i> [cm]	<i>Fraction</i> [μm]	<i>Age group</i> [years]	Δt [years]	ΔSOC $t\ C\ ha^{-1}$	<i>Sequestration rate</i> $t\ C\ ha^{-1}y^{-1}$
0-20	$f_{<2000\ \mu m}$	50-70	60	23.3	0.39
		1-70	38	18.1	0.48
	$f_{2000-200\ \mu m}$	1-70	38	3.9	0.10
	$f_{200-20\ \mu m}$	1-70	38	3.4	0.09
	$f_{<20\ \mu m}$	50-70	60	10.6	0.18
20-40	N.S.				
0-40	$f_{<2000\ \mu m}$	50-70	60	23.0	0.38
	$f_{2000-200\ \mu m}$	50-70	60	7.7	0.13
	$f_{200-20\ \mu m}$	30-45	38	6.0	0.16

3.6 Csat and Cdef

The relationship between the textural fraction of mineral soil in the fine silt and clay fraction ($f_{<20\ \mu m}$) and the associated SOC is a relevant metric persistent SOC status, as it elucidates the $f_{<20\ \mu m}$ SOC saturation level (Hassink, 1997). The average percentage of mineral $f_{<20\ \mu m}$ was $49.2\% \pm 1.3$ and ranged from 27.1% to 70.2% across all sites, land uses and depths, and as can be seen in Figure 3.9. Mineral $f_{<20\ \mu m}$ percentages (x-axis) were within the same range irrespective of land use. A clear trend in the 0-20 cm layer (Figure 3.9a) could be observed in $f_{<20\ \mu m}$ SOC, where hedgerow soils generally exhibited higher $f_{<20\ \mu m}$ SOC concentrations than arable soils (Table 3.2). In the 0-20 cm soil layer, mineral $f_{<20\ \mu m}$ did not correlate significantly with associated SOC concentrations (Figure 3.9a), however a very similar trend was observed for both land use types ($p = 0.07$) indicating a positive correlation between mineral $f_{<20\ \mu m}$ and associated SOC. In the 20-40 cm layer, the correlation was significant in arable soils while an outlier in hedgerow subsoil with SOC concentrations of resulted in a poor correlation (Figure 3.9b).

As shown in Figure 3.10, both C_{sat} and C_{def} stocks tended to be larger in arable soils compared to hedgerow soils. In the 0-20 cm layer, C_{sat} stocks were on average $163 \text{ t C ha}^{-1} \pm 9.2$ in arable and $127 \text{ t C ha}^{-1} \pm 8.4$ in hedgerows. This difference was significant ($p < 0.01$). In the 20-40 cm C_{sat} stocks were generally larger than under cultivation: $180 \text{ t C ha}^{-1} \pm 8.7$ (arable) and $148 \text{ t C ha}^{-1} \pm 16$ (hedgerow), although insignificant ($p = 0.19$). C_{def} stocks exhibited the same trend as for C_{sat} stocks, namely significantly larger under cultivation in comparison to hedgerows in topsoil ($p < 0.01$), but not in subsoil ($p = 0.16$). In line with this, the relative degree of saturation was higher in hedgerow topsoil (34% in 0-20 and 26% in 20-40) compared to arable (26% in 0-20 cm and 23% in 20-40 cm).

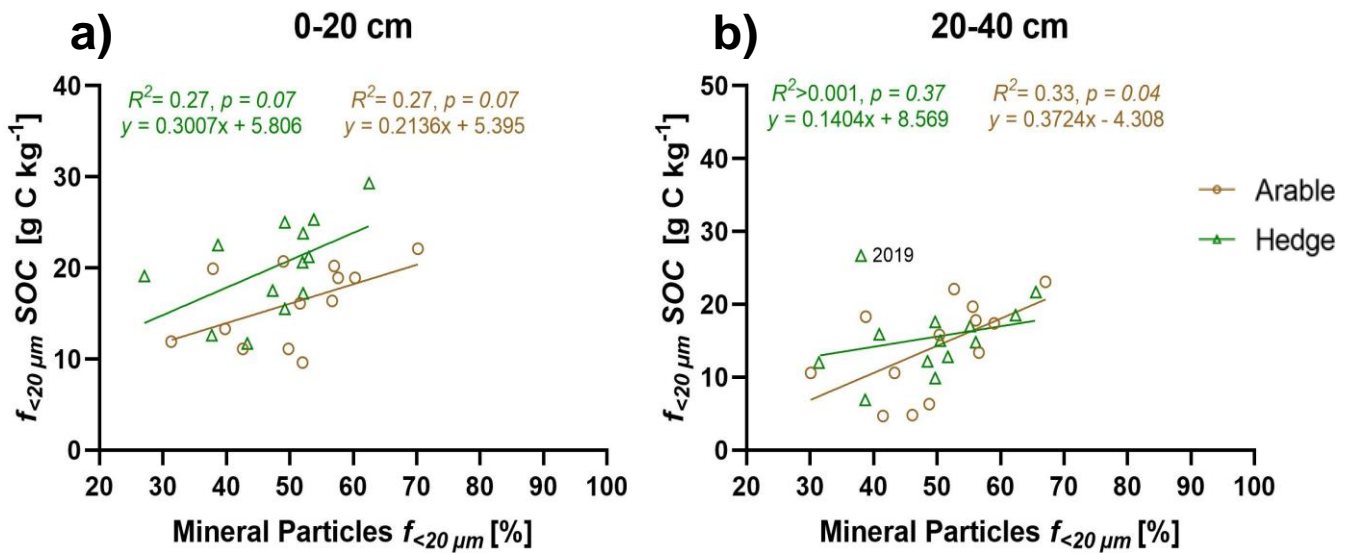


Figure 3.9 Linear regressions of hedgerow and arable SOC in $f_{<20 \mu\text{m}}$ [g C kg^{-1}] as a function of mineral particles in $f_{<20 \mu\text{m}}$: a) In the 0-20 cm soil layer b) 20-40 cm soil layer Coefficients of determination, p-values (at the 0.05 significance level) for a non-zero slope and modelled linear equations are reported for each land use individually.

Furthermore, hedgerow subsoil had significantly higher C_{sat} ($p < 0.001$) and C_{def} ($p < 0.0001$) relative to topsoil. The same pattern could be observed in arable soils, however marginally insignificant for C_{sat} ($p = 0.06$), and significant in terms of C_{def} ($p = 0.03$).

In contrast, C_{sat} concentrations were highly similar in soils grouped by land use and depth varying less than 5% between hedgerow and arable soils in both depth increments (ranging between $62 \text{ g C kg}^{-1} \pm 10$ and $60 \text{ g C kg}^{-1} \pm 11$) (Figure 3.11), . Additionally, no significant differences between land uses were

found in C_{def} concentrations in 0-20 cm ($p = 0.11$), and in 20-40 cm ($p = 0.70$). The only significant difference ($p < 0.01$) was found in C_{def} concentrations between topsoil ($39.1 \text{ g C kg}^{-1} \pm 9.8$) and subsoil ($45.2 \text{ g C kg}^{-1} \pm 10.1$) under hedgerows.

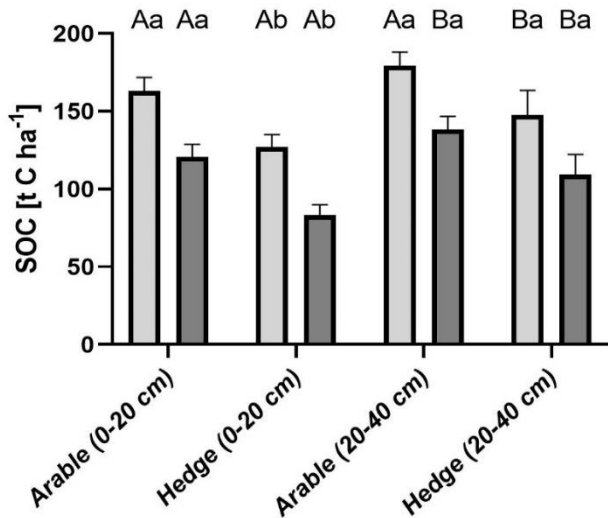


Figure 3.10 Stocks [t C ha^{-1}] of carbon saturation potentials (C_{sat}) and carbon saturation deficits (C_{def}) across depth and land use. Estimates are based on C_{sat} equation derived by Wenzel et al., (2022). Figures are reported in means with SE bars. Uppercase letters indicate depth differences between same land use (paired t-test), while lowercase letters indicate land use differences between same depth increments (unpaired t-test).

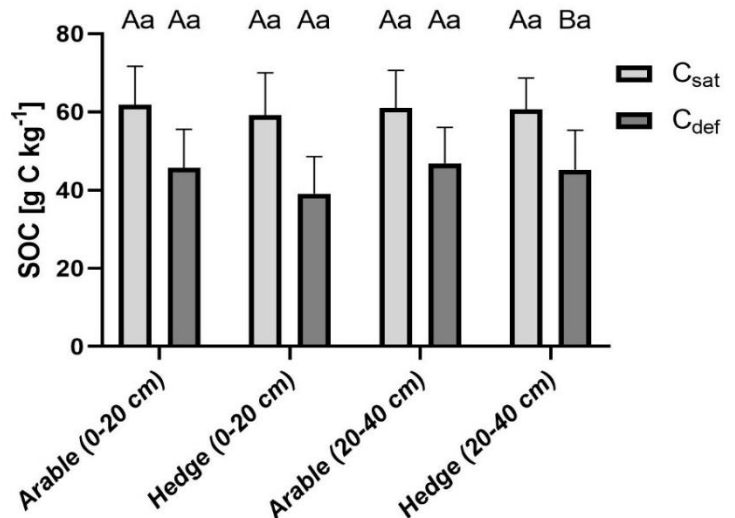


Figure 3.11 Carbon saturation potentials and (C_{sat}) and carbon saturation deficits (C_{def}) across depth and land use. Estimates are based on C_{sat} equation derived by Wenzel et al., (2022). Figures are reported in means with SE bars. Uppercase letters indicate depth differences between same land use (paired t-test), while lowercase letters indicate land use differences between same depth increments (unpaired t-test).

4. Discussion

The space-for-time substitution approach coupled with particle size fractionation allowed for estimations of SOC sequestration and associated sequestration rates. As hypothesized, results indicated that SOC sequestration increased as hedgerows matured, which was particularly evident in SOC fractions resembling partially decomposed plant residues. Clear differences in depth distributions of SOC were observed between the two land uses with implications on the vertical extent of SOC sequestration. Additionally, soils in the study area exhibited high C_{def} values, only slightly affected by hedgerows. Main results will be discussed in further detail in the next sections by including comparable research from the scientific literature to contextualize the findings.

4.1 Depth distribution of SOC

Hedgerow topsoil was the driver of SOC sequestration, while no effects were detected below 20 cm. This is corroborated by the fact that the 0-40 cm sequestration data (sum of topsoil and subsoil) generally followed the 0-20 cm trend. Since subsoil OC-accumulation has been claimed to have a large potential for sequestration (Rumpel and Kögel-Knabner, 2011), the limited subsoil OC accrual observed in this study will now be discussed.

SOC stocks in soils under hedgerows showed a rather steep vertical gradient, as topsoil stored 31% more SOC than subsoil (Figure 3.4). Contrastingly, SOC stocks under cultivation were almost the same in top- and subsoil. One likely reason for the latter is that ploughing of cultivated soils tends to redistribute SOC (e.g., crop residues) from shallow to deeper layers, creating a relatively uniform distribution down to the depth of ploughing (Tebrügge and Düring, 1999). The exact plough depth is not known for the studied cultivated soils, however based on Spiegel et al.,'s (2007) research on effects of tillage in Lower Austria, the ploughing depths of 25-30 cm may be assumed for conventional tillage. It is thus assumed that redistribution of SOC through tillage affected the 20-40 cm depth to some degree and may partly explain the lack of differences between the two depth increments in arable soils.

The more pronounced SOC depth gradient in unploughed soils under hedgerows has several likely causes. First, the limited relocation of organic material from the surface to deeper layers of the soil profile as a result of less effective vertical incorporation processes, such as bioturbation (Jobbágy and Jackson, 2000; Rumpel and Kögel-Knabner, 2011). Similar depth distributions have been found in other

unploughed soil systems such as forest SOC stocks, (Grüneberg et al., 2014), as well as in studies of minimum or no-tillage practices, where SOC accumulation is restricted to the top 10 cm compared to conventional tillage (Meurer et al., 2018). In line with this research, the SOC stocks in the 0-20 cm layer under hedgerows were 38% larger compared to tilled cultivated soils. Besides limited vertical redistribution, higher OM inputs from above ground biomass near the soil surface and contributions from belowground sources such as roots and related rhizodeposition may explain the observed variations (Cardinael et al., 2018).

The insignificant differences in SOC stocks in 20-40 cm, indicate that hedgerows were unable to increase SOC stocks in the former arable subsoil within the timeframe studied here. This result agrees with the insignificant differences in 20-40 cm SOC stocks between hedgerow and arable soils found by Herold (2022). Studies of forest soils also suggest slow subsoil SOC accumulation compared to arable soils, which in part was explained by the only partial incorporation of litter from the forest floor compared to the direct burial of OM in ploughed soils (Bárcena et al., 2014; Alcántara et al., 2017). However, contrasting evidence of subsoil SOC enrichments under comparable conditions is found in the literature. A meta-analysis of SOC sequestration in temperate agroforestry systems, including hedgerows, found a significant relative increase of ~10% between agroforestry systems and arable control soils in the 20-40 cm depth, however lower than increases in 0-20 cm (~15%) (Mayer et al., 2022a). Biffi et al. (2022) found higher SOC sequestration under hedgerows on intensively managed grasslands in 0-50 cm (41.5 t C ha⁻¹) than in 0-30 cm depth (29.5 t C ha⁻¹), indicating subsoil effects of hedgerows. However, the latter study does not report any information on tillage.

In sum, inherent differences in OM inputs and mechanisms of relocation in the compared land uses, influenced observed vertical distribution of SOC sequestration under hedgerows.

4.2 SOC sequestration in bulk soil

Samples used in this study were taken as a subset of a larger sample collection (N=119) of hedgerow-field sites gathered by Herold (2022). It is therefore relevant to compare SOC stocks reported in this study to those found by Herold. In 0-20 cm, Herold found median stocks of 56.1 t C ha⁻¹ (hedgerow) and 50.9 t C ha⁻¹ (arable) compared to mean stocks in this study of 66.0 t C ha⁻¹ ± 4.3 (hedgerow) and 47.9 t C ha⁻¹ ± 2.8 (arable). Higher topsoil SOC stocks under hedgerows may be explained by the ESM

corrections employed in this study, as Herold (2022) calculated stocks on a FD basis. In subsoil, stocks were similar since Herold reported 45.5 t C ha⁻¹ (hedgerow) and 43.7 t C ha⁻¹ (arable) in comparison to 50.4 t C ha⁻¹ ± 5.0 (hedgerow) and 45.8 t C ha⁻¹ ± 4.8 (arable) found in this study. An even larger sample size of arable soils (N = 576) across the entire province of Lower Austria, report lower median SOC stocks than found in this study: 36 t C ha⁻¹ (0-20 cm) and 29 t C ha⁻¹ (20-50 cm) and 66 t C ha⁻¹ (0-50 cm) (Wenzel et al., 2022). These values are, however, overall medians that are taken from the climatically and geologically diverse Lower Austrian region covering a wide range of soils. If only Chernozem and Phaeozems are considered in the data provided by Wenzel et al., (2022), then median SOC stocks are closer to the values reported here (~40 t C ha⁻¹ and ~ 80 t C ha⁻¹ in the 0-20 cm and 0-50 cm depth, respectively). Hence, the relatively small sample size (N=13) investigated in this thesis, reasonably represents SOC in the study area compared to larger, and more representative bodies of data.

In spite of the insignificant linear relationship between hedgerow age and SOC sequestration in $f_{<2000\ \mu\text{m}}$, SOC sequestration rates could still be derived based on average ΔSOC over the whole chronosequence (using average hedgerow age of 38 years) – a common approach when estimating SOC accumulation rates (Grüneberg et al., 2014; Mayer et al., 2022a; Viaud and Kunnemann, 2021; Wenzel et al., 2022). This approach yielded an accumulation rate¹ of 0.48 t C ha⁻¹ y⁻¹ as shown in Table 4 in the results section. This rate is similar to those reported in meta-analyses of agroforestry systems, including but not limited to hedgerows (Cardinael et al., 2017) and of hedgerow land use specifically (Drexler et al., 2021; Mayer et al., 2022a).

Interestingly, Wenzel et al., (2022) found, that arable soils in Lower Austria accumulated SOC in the 0-20 cm (0.21 – 0.43 t C ha⁻¹ y⁻¹) between 1985/2000 and 2015/2020. This was suggested to be the result of legislative changes prohibiting open biomass incinerations and implementing SOC-enhancing measures such as organic cultivation and cover crops. Thus, as burning of straw in fields became illegal and additional C input strategies to arable soils became more widespread, SOC stocks likely increased due to a decreased losses and increased inputs (Wenzel et al., 2022). This simultaneous accumulation in arable soils may have underestimated potential SOC sequestration under hedgerows, compared to other cultivated areas under similar conditions where cropland soils experience net SOC losses (Keel et al.,

¹ It should be noted that two sequestration rates were presented in Table 3.4: 0.48 t C ha⁻¹ y⁻¹ applying $f_{<2000\ \mu\text{m}}$ ΔSOC for the whole chronosequence and 0.39 t C ha⁻¹ y⁻¹ found for old hedgerows (50-70 years). Since the latter only represents the variation in older hedgerows, the former is applied in this discussion as it represents ΔSOC for the whole chronosequence.

2019). Assuming an annual SOC stock increase of $0.32 \text{ t C ha}^{-1} \text{ y}^{-1}$ (average of 0.21 and 0.43) of arable soils topsoil in our study area, from 1985-2019, this would increase the predicted hedgerow sequestration rate by approximately 14% (Figure 4.1). If similar SOC accumulation in topsoil under cultivation would have occurred throughout the temporal range of this study (1950-2019), a substantially larger correction of 66% (Figure 4.1) would be made. However, as Wenzel et al., (2022) provide information on changes occurring in the past 35 years and link these changes to specific management shifts during this period, the latter correction is not backed by scientific evidence, and may merely be an illustration of how a moving baseline can affect such estimations.

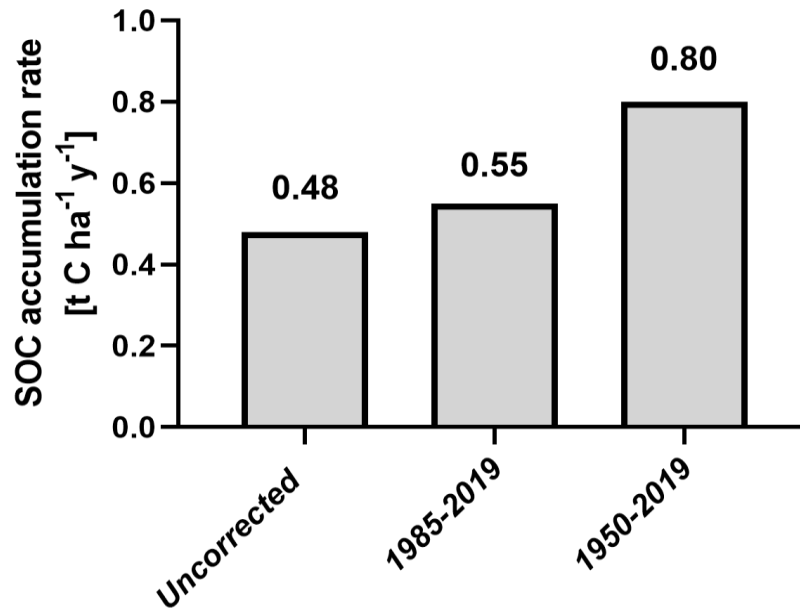


Figure 4.1 Estimations of SOC accumulation rates [t C ha⁻¹ y⁻¹] after hedgerow planting on arable soil in 0-20 cm. “Uncorrected” represents the arable baseline SOC stocks reported in this study, “1985-2019” represents a scenario where arable soils accumulated $0.32 \text{ t C ha}^{-1} \text{ y}^{-1}$ within the age interval indicated by Wenzel et al., (2022) and “1950-2019” represents a scenario where arable soils accumulated $0.32 \text{ t C ha}^{-1} \text{ y}^{-1}$ throughout the entire age interval assessed in this study.

The first hypothesis (H1) stated that bulk SOC stocks ($f_{<2000 \mu\text{m}}$) would increase as a function of hedgerow age compared to adjacent cultivated soils. Or in other words, that hedgerows would sequester $f_{<2000 \mu\text{m}}$ SOC as a function of hedgerow age. In topsoil, ΔSOC in $f_{<2000 \mu\text{m}}$ tended to increase linearly with

hedgerow age, however not significantly ($p = 0.07$, Table 3.3). Additionally, old hedgerows (50-70 years) significantly sequestered SOC ($23.3 \text{ t C ha}^{-1} \pm 5.1$) while younger hedgerows (1-22 years and 30-45 years) did not significantly increase SOC stocks compared to the baseline (Table 3.4). No such trends could be found in the subsoil, which was also reflected in the almost identical sequestration in the 0-40 cm layer under old hedgerows (23.0 t C ha^{-1}). Taken together, this gives an indication that hedgerows sequester additional SOC as stands evolve, though at a rather coarse temporal resolution.

Considering several marginally insignificant results, coupled with a relatively small sample size, it may be expected that more data points would allow for more conclusive results on this matter. Small sample sizes are vulnerable to outliers as illustrated by the oldest hedgerow-field site in this study (70 years), which showed ΔSOC of 5.1 t C ha^{-1} , considerably lower than the mean in the 50-70-year age group 23.3 t C ha^{-1} . Furthermore, a legacy effect from older hedgerow vegetation than that reported by farmers to the district authority's databases, may also have interfered with the ability to observe a clear effect of age. Likewise, a recent study was unable to find an age effect on hedgerow SOC accumulation in grassland soils, attributing this to the presence of old vegetation in sites assumed to be younger (Ford et al., 2019). Similar observations were made for a few hedgerow sites in this study, however most evidently in Figure 3.1c showing a 6-year-old site with several *Prunus* trees >10 meter tall which an unlikely growth rate (Kupka, 2007) and may well be a sign of a legacy effect.

In summation, there was some evidence to support the claims of H1 as only the oldest hedgerows significantly sequestered SOC in topsoil, when grouped by age. Additionally, linear regression analysis provided an indication of continuous increases in ΔSOC as a function of hedgerow age, however not significantly.

4.3 SOC sequestration in particle size fractions

Large relative increases in SOC stocks occurred in coarse fractions: $f_{2000-200 \mu\text{m}}$ (315%) and $f_{200-20 \mu\text{m}}$ (89%). These fractions represent rather modest stocks, thus small absolute changes may produce large relative changes. Considering the limited contribution to $f_{<2000 \mu\text{m}}$ SOC, the absolute changes observed are of more importance (3.85 t C ha^{-1} in $f_{2000-200 \mu\text{m}}$ and 3.37 t C ha^{-1} in $f_{200-20 \mu\text{m}}$). This is further emphasized by the fact that these fractions combined constitute 25.8% of the $f_{<2000 \mu\text{m}}$ SOC, while they contribute ~40% to the SOC stock increases. Substantial accumulation in coarse SOC fractions in topsoil were expected due to the higher inputs of litter and roots of hedgerows compared to the cyclic removal of C from

harvested arable fields. The fact that relative stocks of coarse SOC fractions decreased markedly after 0-20 cm (Table 3.2) is another indication that increased surface litter and shallow roots contribute to this topsoil fraction. Furthermore, as shown in Figure 7c, a positive linear relationship between SOC in $f_{2000-200\ \mu\text{m}}$ and $f_{200-20\ \mu\text{m}}$ was found, suggesting that the accumulation of coarse POM ($f_{2000-200\ \mu\text{m}}$) increased formation of finer POM ($f_{200-20\ \mu\text{m}}$). This finding was in line with the mechanistic understanding of finer POM formation as a product of fragmentation and partial decomposition of coarser POM and litter (Han et al., 2022). This, coupled with the positive correlation between hedgerow age and ΔSOC in the $f_{2000-200\ \mu\text{m}}$, could indicate that additional litter and root derived OM accumulate in mineral soil as hedgerow vegetation matures, and is sequentially broken down into finer fractions. However, evidence that $f_{200-20\ \mu\text{m}}$ SOC accumulates as a function of hedgerow age could not be supported by the data (Table 3.3).

The second hypothesis (H2) claimed that ΔSOC in $f_{<20\ \mu\text{m}}$ would increase with hedgerow age compared to adjacent soils under cultivation as long as $C_{\text{def}} > 0$. Firstly, topsoil ΔSOC in $f_{<20\ \mu\text{m}}$ showed very limited signs of increasing linearly with hedgerow age (Figure 3.7). However, as with $f_{<2000\ \mu\text{m}}$, old hedgerows (50-70 years) significantly sequestered SOC in $f_{<20\ \mu\text{m}}$ as opposed to younger hedgerows (1-22 years and 30-45 years). Thus, while it was not possible to describe a continuous temporal trend of how ΔSOC in $f_{<20\ \mu\text{m}}$ was accrued over time, there was some evidence that sequestration of persistent SOC was taking place under old hedgerows. This is also in line with the marginally insignificant differences between topsoil $f_{<20\ \mu\text{m}}$ SOC stocks under hedgerows and cultivated fields when the chronosequence was considered at large ($p = 0.053$, Table 3.2), indicating a trend of SOC sequestration of persistent SOC.

The incorporation of SOC into the $f_{<20\ \mu\text{m}}$ may to some extent be dependent on the breakdown of larger fractions of organic matter ($f_{2000-200\ \mu\text{m}}$ and $f_{200-20\ \mu\text{m}}$) expected to mineralize within years to decades (Lavallee et al., 2019). As hypothesized by Cotrufo et al. (2012), labile plant material is the primary source of microbial products which in turn are thought to be the main precursor to MAOM, represented in this study by $f_{<20\ \mu\text{m}}$ SOC. Thus, as new labile plant components are incorporated under hedgerows, there may be a delayed effect on increases in the $f_{<20\ \mu\text{m}}$ SOC pool. This effect could have impacted the ability to describe the development of ΔSOC in $f_{<20\ \mu\text{m}}$ linearly over time, however such a time lag would be expected to lie within the timeframe of the chronosequence considered here. Furthermore, evidence of a descending sequential breakdown according to particle size could not be found between $f_{<20\ \mu\text{m}}$ and $f_{2000-200\ \mu\text{m}}$ and $f_{200-20\ \mu\text{m}}$ (Figure 3.6). This relationship may have been partly obscured by the large age

variation of hedgerows when considering the whole chronosequence. Young hedgerow sites may not show strong relationships between fine and coarse fraction SOC due to the time-dependent breakdown pathway from coarser fractions to $f_{<20\ \mu\text{m}}$.

Consequently, the first part of H2 could to a limited degree be corroborated by the data presented, yet a more general prediction of SOC accrual over time is needed.

4.4 C_{sat} and C_{def}

The latter assumption of H2 was that SOC could be sequestered in $f_{<20\ \mu\text{m}}$ as long as the studied soils did not show signs of SOC saturation in $f_{<20\ \mu\text{m}}$ ($C_{\text{def}} < 0$). However, C_{def} , as estimated by the C_{sat} equation derived by Wenzel et al (2022), was far from saturation across all sites, treatments, and depths (Figures 3.10 & 3.11). Firstly, C_{sat} and C_{def} stock estimates were generally larger in subsoil than topsoil for both land uses, and significantly greater in topsoil under cultivation relative to hedgerow topsoil (Figure 3.10). Land use was not expected to alter C_{sat} due to the proximity of the paired samples, which are assumed to be similar in soil mineral particle composition. However mean C_{sat} stocks were 21% larger in arable topsoil compared to hedgerows. Meanwhile estimated mineral particles in $f_{<20\ \mu\text{m}}$ [%] varied very little (2% on average) between hedgerows and arable soils (Table 3.1) and differences are therefore more likely caused by biases in BD. The FD approach was used to calculate the C_{sat} stocks based on BD, which were systematically lower in hedgerow soils, as already shown (Figure 3.2). The influence of BD may be further corroborated by the fact that land use differences in C_{sat} concentrations (calculated independently of BD) were negligible (Figure 3.11). This is similar to findings across various land uses (cropland, forest and grasslands) in Bavarian topsoil (Wiesmeier et al., 2014). Since calculations of C_{def} stocks are inherently related to the magnitude of C_{sat} stocks, C_{def} stock differences between soils under arable land and hedgerows should be interpreted with care. Alternatively, degree of stock saturation may be a better measure of comparison as it is a relative term. Degree of stock saturation were 34 % (hedgerow) and 26 % (cultivated) in topsoil, indicating that hedgerow planting leads to an increased utilization of the soil's protective capacities. This is also in line with the finding that C_{def} concentrations were on average ~13% lower in hedgerow soils (Figure 3.11).

C_{sat} estimates of cultivated topsoil in the study area are lower than estimates of the entire province of Lower Austria (Wenzel et al., 2022). In line with this, relative saturation degrees were higher than in the whole province (20% in the province and 26% in this study). Discrepancies are not surprising due to the different approaches used by Wenzel et al., (2022), who estimated C_{sat} and C_{def} based on soil inventory data of particle size distributions and a fixed factor of 0.85 to estimate $f_{<20 \mu\text{m}}$ SOC (out of $f_{<2000 \mu\text{m}}$). In contrast, this study applied a fractionation method qualifying the 0.85 factor (Figure 3.5) and did not include an independent mineral particle size distribution procedure. However, the fact that the $f_{<20 \mu\text{m}}$ SOC constituted a lower relative amount in $f_{<2000 \mu\text{m}}$ in hedgerow topsoil (~0.75) indicates that such factors could be estimated for different land uses to avoid overestimations of C_{sat} .

The estimated mean saturation degree of 34 % in topsoil under hedgerows is still far from saturation and begs the question: Are C_{sat} estimations realistic? Wenzel et al.'s (2022) equation may overestimate C_{sat} in this study for at least two reasons. Firstly, a large share of the grassland data used by Wenzel et al. (2022) were from areas in Lower Austria that generally receive more precipitation than the relatively dry Pannonian region (this study, see site description in methods section). Increased plant available water may in turn lead to more productive plant communities, capable of increasing above- and belowground OM input to stimulate SOM formation. Secondly, it has been shown that grasslands have higher root:shoot ratio biomass distributions than ecosystems dominated by woody species (Qi et al., 2019). Hence, in grassland ecosystems, more SOC enter soils in the rhizosphere, favorable for the buildup persistent SOM via direct pathways for microaggregate formation and interactions with soil minerals (Rasse et al., 2005; Kleber et al., 2015). This highlights the suitability of grasslands as a benchmark land use for estimation of maximal SOC in $f_{<20 \mu\text{m}}$ in C_{sat} equations but may explain in part why hedgerows are still far from saturation. On this note it is important to stress that grassland management varies which affects SOC stocks (Conant et al., 2017). Furthermore, the importance of other constituting elements of SOM, such as N, P and S have been emphasized as a limiting factor for SOM formation and thus SOC sequestration (Kirkby et al., 2014).

Finally, the notion that $f_{<20 \mu\text{m}}$ SOC could be sequestered to the point of full saturation (H2) was not reflected by the data reported in this study. Mean saturation level in topsoil on average increased from 26% to 34% after hedgerow planting, which either indicates that hedgerows show a limited potential to decreased C_{def} levels, or that modelled C_{sat} is overestimated. Moreover, even if C_{sat} values are

overestimated to some degree, it would appear that soils under cultivation in the study area show a potential for further sequestration or storage of persistent SOC.

4.5 Implications of C_{sat} model choice

While this study was privileged by the availability of a C_{sat} model parameterized using data from near the study area, several other C_{sat} models exist. One such model, derived by Hassink (1997) has been broadly applied (Angers et al., 2011; Wiesmeier et al., 2014). In the following, the implications of the choice of C_{sat} model will be discussed by comparing C_{sat} and C_{def} estimations using the equations of Wenzel et al., (2022) and Hassink (1997).

Figure 4.2 shows the $f_{<20\mu m}$ SOC status according to the different C_{sat} regression models as reported by Hassink (1997) and Wenzel et al., (2022). In topsoil, Hassink's equation estimates the average C_{def} values to be 6.6 g C kg⁻¹ (cultivated) and 1.8 g C kg⁻¹ (hedgerows), where 5 out of 13 hedgerow soils exhibited negative C_{def}-values, suggesting oversaturation. In comparison, Wenzel's equation estimated C_{def} to be 45.7 g C kg⁻¹ (cultivated) and 39.1 g C kg⁻¹ (hedgerows). There are several explanations for these substantial differences. Firstly, the Hassink equation is based on global data that inevitably represent climatic regions very different from this study area – an influencing factor on SOC storage (Wiesmeier et al., 2019). Additionally, Hassink's equation was obtained using a LS regression which inherently creates a line that minimizes SSE for all data points, thus producing a measure of the mean C_{sat} (Feng et al., 2013). Since such a “best fit for all” line is likely to also represent soils that are not saturated, Feng et al., (2013) proposed to use a boundary line (BL) regression approach, that only considers the upper tenth percentile of data points (assumed to be closer to saturation) to prevent underestimation of C_{sat}. Wenzel et al., (2022) also uses a BL (90th percentile) and this approach produced substantially larger slopes resulting in higher C_{sat} estimates.

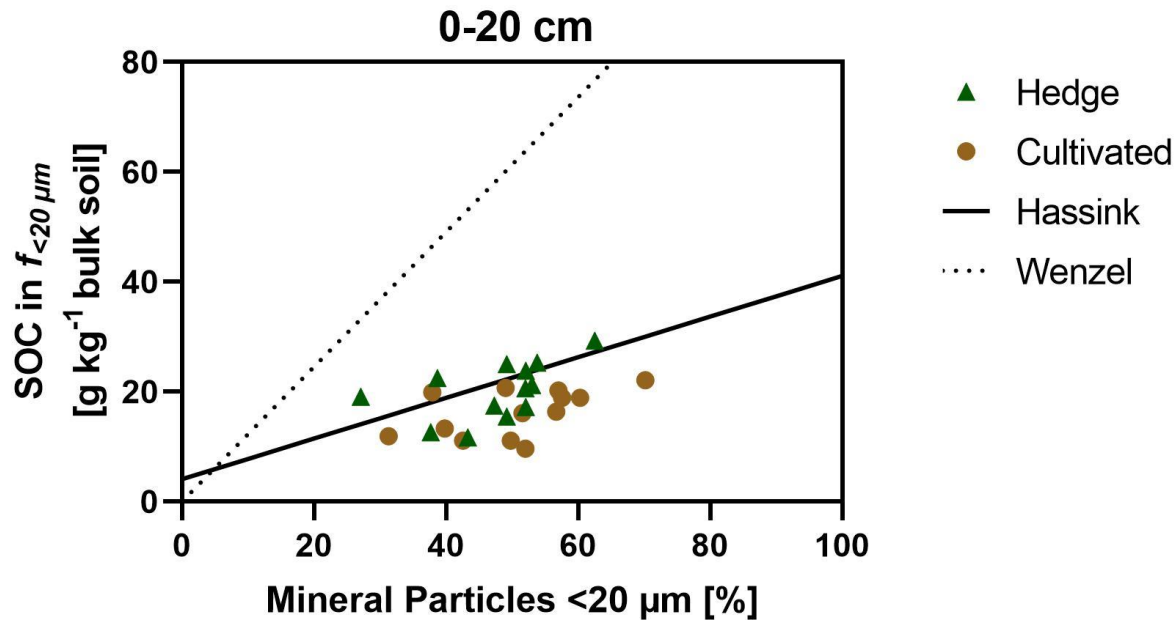


Figure 4.2 Relationships between SOC in $f_{<20 \mu m}$ [g C kg⁻¹ $f_{<2000 \mu m}$ soil] and proportion of mineral particles <20 μm for hedgerows and cultivated topsoil with C_{sat} curves from Hassink ($y= 4.09x + 0.37$) and Wenzel et al., ($y=1.227x$).

Consequently, if Hassink’s equation would have been used to interpret C_{def} , the conclusion would have been highly different. Namely, that the cultivated soils in the study area were already relatively close to saturation, and that hedgerows show a potential to fully saturate them with persistent SOC. This demonstrates the importance of local C_{sat} models, which has also been stressed by others (e.g. Paterson et al., 2021). With this being said, as indicated in the previous discussion, even models based on local data are still not local enough and should be viewed as a theoretical maximum, not necessarily attainable in practice.

4.5 Hedgerow planting as climate change mitigation

One goal of the EU Biodiversity Strategy for 2030 is to ensure that at least 10% of agricultural land consists of high-diversity landscape features, where hedgerows are mentioned as an example (European Commission, 2021). If 10% of the cultivated area of Lower Austria, that is 68,285 ha in 2016 (Wenzel et al., 2022) were to be converted into hedgerow vegetation, and the mean accumulation rate (0.48 t C ha⁻¹ y⁻¹) found in this study was assumed for the whole province, it would amount to a CO₂-sequestration

of $\sim 120 \text{ Gg CO}_2 \text{ y}^{-1}$ (or $0.12 \text{ Tg CO}_2 \text{ y}^{-1}$). The total annual CO_2 -emissions of Lower Austria are estimated to be $\sim 15 \text{ Tg y}^{-1}$ (Anderl et al., 2017) thus only compensating for 0.8% of the total emissions, taking ~ 125 years to compensate for the emissions of just one year.

On a global scale, the “4 per mille initiative” was an action program established during COP21, aimed to compensate global anthropogenic GHG emissions by increasing global SOC stocks by 0.4% per year. The 0.4% sequestration rate stems from estimations of annual GHG emissions deriving from fossil carbon of 8.9 Gt C relative to global SOC stocks (down to 200 cm) of 2400 Gt C (Batjes, 1996), that is $8.9/2400 = 0.4\%$. The ambition of the 4 per mille initiative has been challenged several times in the scientific literature. Specifically for being unrealistic in terms of carbon sequestration potentials of non-agricultural soils with high baseline SOC, the feasibility of monitoring SOC stocks down to 200 cm (which is rarely sampled) as well as questions relating to the necessary sources of other SOM forming constituents, such as nitrogen (Minasny et al., 2017; van Groenigen et al., 2017; VandenBygaart, 2018). The debate has given rise to more conservative estimates of expected outcomes of the 4 per mille initiative. Minasny et al., (2017) has for example suggested that annual SOC increases of 0.4% may compensate 30% of global GHG emissions, while VandenBygaart (2018) provided an even more conservative estimate of 5-10%.

In this study, a SOC sequestration rate of $0.48 \text{ t C ha}^{-1} \text{ y}^{-1}$ is equivalent to $\sim 1\%$ annual increases in soils under cultivation ($0.48/47.9 = \sim 1\%$). While this is more than double a 0.4% increase, such accumulations only occurred in the top 20 cm layer of soil. It has been estimated by others, that the top 30 cm of soil store $\sim 50\%$ of SOC in the uppermost 100 cm and $\sim 30\%$ in the uppermost 200 cm (Batjes 1996). Therefore, a $1\% \text{ y}^{-1}$ SOC stock increase in the 0-20 cm would equal $<0.5\% \text{ y}^{-1}$ and $<0.3\% \text{ y}^{-1}$ when considered on a 100 cm or 200 cm soil layer basis. Hence, a $0.4\% \text{ y}^{-1}$ in 200 cm, as the initial goal set out to achieve, would entail $\sim 1.3\% \text{ y}^{-1}$ in the 0-30 cm. Nevertheless, as stressed by Minasny et al., (2018); 4 per mille is not a magic number but “*a worthy aspirational target that has also become a slogan in helping the promotion of sustainable soil management and global soil security*” (p. 125).

In summary, relying on hedgerow establishment on agricultural soil for a full compensation of CO_2 -emissions in Lower Austria does not seem feasible, and should not be used as a means to delay other

mitigation measures. With this being said, one should not overlook the possible synergy of other ecosystem functions that hedgerows may deliver outside the scope of this thesis.

5. Concluding remarks

SOC sequestration of cultivated soils may play an important part in reaching net-zero GHG-emissions if potentials are realized. Thus, quantifying SOC sequestration and storage enhancements from different sources based on in-situ evidence is needed to identify the most effective measures. In this thesis, sequestration potential of hedgerows in the intensively cultivated dry Pannonian region of Lower Austria was examined. By establishing a chronosequence of field-bordering hedgerows planted between 1950 and 2019, multi-decadal SOC stock evolution was modelled. Moreover, separation of SOC components into fractions of varying persistence was obtained to evaluate long-term implications.

The results show that bulk ($f_{<2000\mu m}$) SOC stocks increased on average by 38% in topsoil after hedgerow planting. SOC sequestration was restricted to the top 20 cm of soil and no effects could be observed in 20-40 cm, which was partly attributed to the influences of tillage in soils under cultivation. Consequently, SOC sequestration in the total depth from 0-40 cm could not be significantly observed on average. Furthermore, through a space-for-time substitution approach, it was shown that topsoil SOC sequestration tended to increase concurrent with hedgerow age. This was informed by a linear trend, and by the observation that >50 years were the only age category to individually sequester SOC significantly (23.3 t C ha^{-1}), which was also reflected in significant sequestration under old hedgerows in the 0-40 cm. Over the entire chronosequence, topsoil SOC sequestration rate was estimated to be $0.48 \text{ t C ha}^{-1} \text{ y}^{-1}$. Consequently, H1 positing that SOC stocks under hedgerows would increase as a function of hedgerow age compared to adjacent soils under cultivation, was corroborated by the results.

Particle size fractionation of soil samples allowed for distinctions between three SOC fractions: $f_{2000-200\mu m}$ and $f_{200-20\mu m}$ representing SOC in relatively unprotected POM and $f_{<20\mu m}$ as a proxy for persistent MAOM. Hedgerow topsoil stored a higher proportion of SOC in POM (24.8%) compared to soils under cultivation (12.1%) while the majority of SOC was stored in MAOM in both land uses (75.2% under hedgerows, 87.7% under cultivated). Of the 38% bulk SOC stock increase, approx. 40% of the sequestration occurred in POM while the remaining was assumed to occur in the persistent $f_{<20\mu m}$. Hence, a noteworthy amount of SOC under hedgerows sequestered in unprotected fractions, vulnerable to management changes. SOC in $f_{2000-200\mu m}$ and $f_{200-20\mu m}$ was correlated with hedgerow age, while not in $f_{<20\mu m}$ SOC, indicating that temporal variations in POM was a driving factor for the linear age trend observed in bulk

SOC sequestration. However, the oldest hedgerows were the only age category to significantly sequester SOC in $f_{<20\ \mu\text{m}}$, suggesting some dependency on stand age.

Based on C_{sat} and C_{def} modelling, degree of SOC stock saturation in topsoil was estimated to increase from 26% under cultivation to 34% under hedgerows. While several sources of possible overestimation of C_{sat} was discussed, the results suggest that cultivated soils of eastern Lower Austria constitute a large unfulfilled storage potential of persistent SOC in $f_{<20\ \mu\text{m}}$. H2, hypothesized that SOC in $f_{<20\ \mu\text{m}}$ under hedgerows would increase concurrently with increasing hedgerow age compared to adjacent soils under cultivation if soils did not reach saturation ($C_{\text{def}} > 0$). While the results indicated that SOC was sequestered in $f_{<20\ \mu\text{m}}$, there was limited evidence to support a gradual effect of hedgerow age on sequestration of persistent SOC, even though soils were never close to saturation.

Furthermore, this study emphasizes the importance of acquiring sufficient knowledge of baseline SOC dynamics to critically assess the assumption of steady state conditions. Especially if management practices differ among baseline sites of a chronosequence. As shown, concurrent changes in the baseline SOC can substantially influence sequestration rate estimations. Additionally, it was evident that more samples are needed to confirm the trends outlined in this thesis as well as deeper sampling to assess sequestration in soil layers completely unaffected by tillage.

Overall, hedgerows show a potential to sequester both bulk and persistent SOC in agricultural landscapes that are generally SOC-depleted. The direct transfer of atmospheric C into soil provided by hedgerows is a contributing factor to climate change mitigation. However, large apparent C_{def} in soils under cultivation in the study area calls for additional C-inputs from various sources to offset CO₂ emissions. Taken together with their provisioning of important ecosystem services, hedgerows constitute important landscape features that should be protected and promoted in the future.

6. References

- Amelung, W., Zech, W., 1999. Minimisation of organic matter disruption during particle-size fractionation of grassland epipedons. *Geoderma* 92, 73–85. [https://doi.org/10.1016/S0016-7061\(99\)00023-3](https://doi.org/10.1016/S0016-7061(99)00023-3)
- Anderl, M., Gangl, M., Haider, S., Ibesich, N., Lampert, C., Moosmann, L., Poupa, S., Purzner, M., Schieder, W., Thielen, P., Titz, M., Zeichmeister, A., 2017. Bundesländer Luftschadstoffinventur 1990–2015. Regionalisierung der nationalen Emissionsdaten auf Grundlage von EU-Berichtspflichten UBA Report REP-0632.
- Angers, D.A., Arrouays, D., Saby, N.P.A., Walter, C., 2011. Estimating and mapping the carbon saturation deficit of French agricultural topsoils: Carbon saturation of French soils. *Soil Use and Management* 27, 448–452. <https://doi.org/10.1111/j.1475-2743.2011.00366.x>
- Axe, M.S., Grange, I.D., Conway, J.S., 2017. Carbon storage in hedge biomass—A case study of actively managed hedges in England. *Agriculture, Ecosystems & Environment* 250, 81–88. <https://doi.org/10.1016/j.agee.2017.08.008>
- Batjes, N. h., 1996. Total carbon and nitrogen in the soils of the world. *European Journal of Soil Science* 47, 151–163. <https://doi.org/10.1111/j.1365-2389.1996.tb01386.x>
- Batjes, N.H., 2014. Total carbon and nitrogen in the soils of the world. *European Journal of Soil Science* 65, 10–21. https://doi.org/10.1111/ejss.12114_2
- Baudry, J., Bunce, R.G.H., Burel, F., 2000. Hedgerows: An international perspective on their origin, function and management. *Journal of Environmental Management* 60, 7–22. <https://doi.org/10.1006/jema.2000.0358>
- Blume, H.P., Brümmer, G.W., Fleige, H., Horn, R., Kandeler, E., Kögel-Knabner, I., Kretschmar, R., Stahr, K., Wilke, B.M., 2016a. Soil Organic Matter. In: Blume H.P. et al (eds) Scheffer/Schachtschabel Soil Science. Springer Berlin Heidelberg, Berlin, Heidelberg. <https://doi.org/10.1007/978-3-642-30942-7>
- Blume, H.P., Brümmer, G.W., Fleige, H., Horn, R., Kandeler, E., Kögel-Knabner, I., Kretschmar, R., Stahr, K., Wilke, B.M., 2016b. Physical Properties and Processes. In: Blume H.P. et al (eds) Scheffer/Schachtschabel Soil Science. Springer Berlin Heidelberg, Berlin, Heidelberg. <https://doi.org/10.1007/978-3-642-30942-7>
- Cardinael, R., Chevallier, T., Cambou, A., Béral, C., Barthès, B.G., Dupraz, C., Durand, C., Kouakoua, E., Chenu, C., 2017. Increased soil organic carbon stocks under agroforestry: A survey of six different sites in France. *Agriculture, Ecosystems & Environment* 236, 243–255. <https://doi.org/10.1016/j.agee.2016.12.011>
- Chenu, C., Angers, D.A., Barré, P., Derrien, D., Arrouays, D., Balesdent, J., 2019. Increasing organic stocks in agricultural soils: Knowledge gaps and potential innovations. *Soil and Tillage Research* 188, 41–52. <https://doi.org/10.1016/j.still.2018.04.011>
- Conant, R.T., Cerri, C.E.P., Osborne, B.B., Paustian, K., 2017. Grassland management impacts on soil carbon stocks: a new synthesis. *Ecological Applications* 27, 662–668. <https://doi.org/10.1002/eap.1473>
- Cotrufu, M.F., Wallenstein, M.D., Boot, C.M., 2012. The Microbial Efficiency-Matrix Stabilization (MEMS) framework integrates plant litter decomposition with soil organic matter stabilization: do labile plant inputs form stable soil organic matter? *Global Change Biology* 8, 988–995. <https://doi.org/10.1111/gcb.12113>
- De Stefano, A., Jacobson, M.G., 2017. Soil carbon sequestration in agroforestry systems: a meta-analysis. *Agroforestry Systems* 92, 285–299. <https://doi.org/10.1007/s10457-017-0147-9>

- de Vries, W., 2018. Soil carbon 4 per mille: a good initiative but let's manage not only the soil but also the expectations: Comment on Minasny et al. (2017) *Geoderma* 292: 59–86. *Geoderma* 309, 111–112. <https://doi.org/10.1016/j.geoderma.2017.05.023>
- Drexler, S., Gensior, A., Don, A., 2021. Carbon sequestration in hedgerow biomass and soil in the temperate climate zone. *Regional Environmental Change* 21, 74. <https://doi.org/10.1007/s10113-021-01798-8>
- Dynarski, K.A., Bossio, D.A., Scow, K.M., 2020. Dynamic Stability of Soil Carbon: Reassessing the "Permanence" of Soil Carbon Sequestration. *Frontiers in Environmental Science* 8, 14. <https://doi.org/10.3389/fenvs.2020.514701>
- Ellert, B.H., Bettany, J.R., 1995. Calculation of organic matter and nutrients stored in soils under contrasting management regimes. *Canadian Journal of Soil Science* 75, 529–538. <https://doi.org/10.4141/cjss95-075>
- European Commission, 2021. EU biodiversity strategy for 2030 : bringing nature back into our lives. Publications Office of the European Union, LU. <https://doi.org/10.2779/677548>
- Feng, W., Plante, A.F., Six, J., 2013. Improving estimates of maximal organic carbon stabilization by fine soil particles. *Biogeochemistry* 112, 81-93. <https://doi.org/10.1007/s10533-011-9679-7>
- Foley, J.A., Ramankutty, N., Brauman, K.A., Cassidy, E.S., Gerber, J.S., Johnston, M., Mueller, N.D., O'Connell, C., Ray, D.K., West, P.C., Balzer, C., Bennett, E.M., Carpenter, S.R., Hill, J., Monfreda, C., Polasky, S., Rockström, J., Sheehan, J., Siebert, S., Tilman, D., Zaks, D.P.M., 2011. Solutions for a cultivated planet. *Nature* 478, 337–342. <https://doi.org/10.1038/nature10452>
- Ford, H., Healey, J.R., Webb, B., Pagella, T.F., Smith, A.R., 2019. How do hedgerows influence soil organic carbon stock in livestock-grazed pasture? *Soil Use and Management* 35, 576-584. <https://doi.org/10.1111/sum.12517>
- Friedlingstein, P., O'Sullivan, M., Jones, M.W., Andrew, R.M., Hauck, J., Olsen, A., Peters, G.P., Peters, W., Pongratz, J., Sitch, S., Le Quéré, C., Canadell, J.G., Ciais, P., Jackson, R.B., Alin, S., Aragão, L.E.O.C., Arneeth, A., Arora, V., Bates, N.R., Becker, M., Benoit-Cattin, A., Bittig, H.C., Bopp, L., Bultan, S., Chandra, N., Chevallier, F., Chini, L.P., Evans, W., Florentie, L., Forster, P.M., Gasser, T., Gehlen, M., Gilfillan, D., Gkritzalis, T., Gregor, L., Gruber, N., Harris, I., Hartung, K., Haverd, V., Houghton, R.A., Ilyina, T., Jain, A.K., Joetzjer, E., Kadono, K., Kato, E., Kitidis, V., Korsbakken, J.I., Landschützer, P., Lefèvre, N., Lenton, A., Lienert, S., Liu, Z., Lombardozi, D., Marland, G., Metzl, N., Munro, D.R., Nabel, J.E.M.S., Nakaoka, S.-I., Niwa, Y., O'Brien, K., Ono, T., Palmer, P.I., Pierrot, D., Poulter, B., Resplandy, L., Robertson, E., Rödenbeck, C., Schwinger, J., Séférian, R., Skjelvan, I., Smith, A.J.P., Sutton, A.J., Tanhua, T., Tans, P.P., Tian, H., Tilbrook, B., van der Werf, G., Vuichard, N., Walker, A.P., Wanninkhof, R., Watson, A.J., Willis, D., Wiltshire, A.J., Yuan, W., Yue, X., Zaehle, S., 2020. Global Carbon Budget 2020. *Earth System Science Data* 12, 3269–3340. <https://doi.org/10.5194/essd-12-3269-2020>
- Grüneberg, E., Ziche, D., Wellbrock, N., 2014. Organic carbon stocks and sequestration rates of forest soils in Germany. *Global Change Biology* 20, 2644–2662. <https://doi.org/10.1111/gcb.12558>
- Haase, D., Fink, J., Haase, G., Ruske, R., Pécsi, M., Richter, H., Altermann, M., Jäger, K.-D., 2007. Loess in Europe—its spatial distribution based on a European Loess Map, scale 1:2,500,000. *Quaternary Science Reviews* 26, 1301–1312. <https://doi.org/10.1016/j.quascirev.2007.02.003>
- Haddaway, N.R., Brown, C., Eales, J., Eggers, S., Josefsson, J., Kronvang, B., Randall, N.P., Uusi-Kamppa, J., 2018. The multifunctional roles of vegetated strips around and

- within agricultural fields. *Environmental Evidence* 7, 14.
<https://doi.org/10.1186/s13750-018-0126-2>
- Han, L., Sun, K., Jin, J., Xing, B., 2016. Some concepts of soil organic carbon characteristics and mineral interaction from a review of literature. *Soil Biology and Biochemistry* 94, 107–121. <https://doi.org/10.1016/j.soilbio.2015.11.023>
- Han, S., Wang, E., Chen, X., Fu, Y., 2022. Accumulation of SOM fractions to croplands and plantations converted from cropland with black soil. *Land Degradation & Development* 33, 638–648. <https://doi.org/10.1002/ldr.4187>
- (Han) Weng, Z., Van Zwieten, L., Singh, B.P., Tavakkoli, E., Joseph, S., Macdonald, L.M., Rose, T.J., Rose, M.T., Kimber, S.W.L., Morris, S., Cozzolino, D., Araujo, J.R., Archanjo, B.S., Cowie, A., 2017. Biochar built soil carbon over a decade by stabilizing rhizodeposits. *Nature Climate Change* 7, 371–376.
<https://doi.org/10.1038/nclimate3276>
- Hassink, J., 1997. The capacity of soils to preserve organic C and N by their association with clay and silt particles. *Plant and Soil* 191, 77–87.
<https://doi.org/10.1023/A:1004213929699>
- Heath, S.K., Soykan, C.U., Velas, K.L., Kelsey, R., Kross, S.M., 2017. A bustle in the hedgerow: Woody field margins boost on farm avian diversity and abundance in an intensive agricultural landscape. *Biological Conservation* 212, 153–161.
<https://doi.org/10.1016/j.biocon.2017.05.031>
- Holden, J., Grayson, R.P., Berdeni, D., Bird, S., Chapman, P.J., Edmondson, J.L., Firbank, L.G., Helgason, T., Hodson, M.E., Hunt, S.F.P., Jones, D.T., Lappage, M.G., Marshall-Harries, E., Nelson, M., Prendergast-Miller, M., Shaw, H., Wade, R.N., Leake, J.R., 2019. The role of hedgerows in soil functioning within agricultural landscapes. *Agriculture, Ecosystems & Environment* 273, 1–12.
<https://doi.org/10.1016/j.agee.2018.11.027>
- IUSS Working Group WRB., 2015. World Reference Base for Soil Resources 2014, update 2015 International soil classification system for naming soils and creating legends for soil maps (No. 106), World Soil Resources Reports. FAO, Rome.
- Jahn, R., Blume, H.P., Asio, V.B., Spaargaren, O., Schad, P., 2006. Guidelines for soil description, 4th edition. FAO, Rome.
- Juvinyà, C., LotfiParsa, H., Sauras-Yera, T., Rovira, P., 2021. Carbon sequestration in Mediterranean soils following afforestation of abandoned crops: Biases due to changes in soil compaction and carbonate stocks. *Land Degradation & Development* 32, 4300–4312. <https://doi.org/10.1002/ldr.4037>
- Keel, S.G., Anken, T., Büchi, L., Chervet, A., Fliessbach, A., Flisch, R., Huguenin-Elie, O., Mäder, P., Mayer, J., Sinaj, S., Sturny, W., Wüst-Galley, C., Zihlmann, U., Leifeld, J., 2019. Loss of soil organic carbon in Swiss long-term agricultural experiments over a wide range of management practices. *Agriculture, Ecosystems & Environment* 286, 106654. <https://doi.org/10.1016/j.agee.2019.106654>
- Keesstra, S.D., Bouma, J., Wallinga, J., Tittonell, P., Smith, P., Cerdà, A., Montanarella, L., Quinton, J.N., Pachepsky, Y., van der Putten, W.H., Bardgett, R.D., Moolenaar, S., Mol, G., Jansen, B., Fresco, L.O., 2016. The significance of soils and soil science towards realization of the United Nations Sustainable Development Goals. *Soil* 2, 111–128. <https://doi.org/10.5194/soil-2-111-2016>
- Kleber, M., Eusterhues, K., Keiluweit, M., Mikutta, C., Mikutta, R., Nico, P.S., 2015. Mineral–Organic Associations: Formation, Properties, and Relevance in Soil Environments, in: *Advances in Agronomy*. Elsevier, p. 1–140.
<https://doi.org/10.1016/bs.agron.2014.10.005>

- Kleber, M., Nico, P.S., Plante, A., Filley, T., Kramer, M., Swanston, C., Sollins, P., 2011. Old and stable soil organic matter is not necessarily chemically recalcitrant: implications for modeling concepts and temperature sensitivity: Slow turnover of labile soil organic matter. *Global Change Biology* 17, 1097–1107. <https://doi.org/10.1111/j.1365-2486.2010.02278.x>
- Kristensen, S.B.P., Busck, A.G., van der Sluis, T., Gaube, V., 2016. Patterns and drivers of farm-level land use change in selected European rural landscapes. *Land Use Policy* 57, 786–799. <https://doi.org/10.1016/j.landusepol.2015.07.014>
- Kupka, I., 2007. Growth reaction of young wild cherry (*Prunus avium* L.) trees to pruning. *Journal of Forest Science* 53, 555–560. <https://doi.org/10.17221/2165-JFS>
- Lal, R., 2018. Digging deeper: A holistic perspective of factors affecting soil organic carbon sequestration in agroecosystems. *Global Change Biology* 24, 3285–3301. <https://doi.org/10.1111/gcb.14054>
- Lal, R., 2004. Soil carbon sequestration impacts on global climate change and food security. *Science* 304, 1623–1627. <https://doi.org/10.1126/science.1097396>
- Laura, V.V., Bert, R., Steven, B., Pieter, D.F., Victoria, N., Paul, P., Kris, V., 2017. Ecosystem service delivery of agri-environment measures: A synthesis for hedgerows and grass strips on arable land. *Agriculture, Ecosystems & Environment* 244, 32–51. <https://doi.org/10.1016/j.agee.2017.04.015>
- Lavallee, J.M., Soong, J.L., Cotrufo, M.F., 2019. Conceptualizing soil organic matter into particulate and mineral-associated forms to address global change in the 21st century. *Global Change Biology* 26, 261–273. <https://doi.org/10.1111/gcb.14859>
- Lehmann, J., Kleber, M., 2015. The contentious nature of soil organic matter. *Nature* 528, 60–68. <https://doi.org/10.1038/nature16069>
- Lemke, R.L., VandenBygaart, A.J., Campbell, C.A., Lafond, G.P., Grant, B., 2010. Crop residue removal and fertilizer N: Effects on soil organic carbon in a long-term crop rotation experiment on a Udic Boroll. *Agriculture, Ecosystems & Environment* 135, 42–51. <https://doi.org/10.1016/j.agee.2009.08.010>
- Lorenz, K., Lal, R., 2014. Soil organic carbon sequestration in agroforestry systems. A review. *Agronomy for Sustainable Development* 34, 443–454. <https://doi.org/10.1007/s13593-014-0212-y>
- Mayer, S., Wiesmeier, M., Sakamoto, E., Hübner, R., Cardinael, R., Kühnel, A., Kögel-Knabner, I., 2022a. Soil organic carbon sequestration in temperate agroforestry systems – A meta-analysis. *Agriculture, Ecosystems & Environment* 323, 107689. <https://doi.org/10.1016/j.agee.2021.107689>
- McCann, T., Cooper, A., Rogers, D., McKenzie, P., McErlean, T., 2017. How hedge woody species diversity and habitat change is a function of land use history and recent management in a European agricultural landscape. *Journal of Environmental Management* 196, 692–701. <https://doi.org/10.1016/j.jenvman.2017.03.066>
- Millar, R.J., Fuglestvedt, J.S., Friedlingstein, P., Rogelj, J., Grubb, M.J., Matthews, H.D., Skeie, R.B., Forster, P.M., Frame, D.J., Allen, M.R., 2017. Emission budgets and pathways consistent with limiting warming to 1.5 °C. *Nature Geoscience* 10, 741–747. <https://doi.org/10.1038/ngeo3031>
- Minasny, B., Arrouays, D., McBratney, Alex.B., Angers, D.A., Chambers, A., Chaplot, V., Chen, Z.-S., Cheng, K., Das, B.S., Field, D.J., Gimona, A., Hedley, C., Hong, S.Y., Mandal, B., Malone, B.P., Marchant, B.P., Martin, M., McConkey, B.G., Mulder, V.L., O'Rourke, S., Richer-de-Forges, A.C., Odeh, I., Padarian, J., Paustian, K., Pan, G., Poggio, L., Savin, I., Stolbovoy, V., Stockmann, U., Sulaeman, Y., Tsui, C.-C., Vågen, T.-G., van Wesemael, B., Winowiecki, L., 2018. Rejoinder to Comments on

- Minasny et al., 2017 Soil carbon 4 per mille *Geoderma* 292, 59–86. *Geoderma* 309, 124–129. <https://doi.org/10.1016/j.geoderma.2017.05.026>
- Minasny, B., Malone, B.P., McBratney, A.B., Angers, D.A., Arrouays, D., Chambers, A., Chaplot, V., Chen, Z.-S., Cheng, K., Das, B.S., Field, D.J., Gimona, A., Hedley, C.B., Hong, S.Y., Mandal, B., Marchant, B.P., Martin, M., McConkey, B.G., Mulder, V.L., O'Rourke, S., Richer-de-Forges, A.C., Odeh, I., Padarian, J., Paustian, K., Pan, G., Poggio, L., Savin, I., Stolbovoy, V., Stockmann, U., Sulaeman, Y., Tsui, C.-C., Vagen, T.-G., van Wesemael, B., Winowiecki, L., 2017. Soil carbon 4 per mille. *Geoderma* 292, 59–86. <https://doi.org/10.1016/j.geoderma.2017.01.002>
- Nestroy, O., Aust, G., Blum, W.E.H., Englisch, M., Hager, H., Herzberger, E., Kilian, W., Nelhiebel, P., Pecina, E., Pehamberger, A., Schneider, W., Wagner, J., 2011. Systematische Gliederung der Böden Österreichs Österreichische Bodensystematik 2000 in der revidierten Fassung von 2011. Österreichische Bodenkundliche Gesellschaft, Wien.
- O'Connell, P.E., Beven, K.J., Carney, J.N., Clements, R.O., Ewen, J., Fowler, H., Harris, G.L., Hollis, J., Morris, J., O'Donnell, G.M., Packman, J.C., Parkin, A., Quinn, P.F., Rose, S.C., Shepherd, M., Tellier, S., 2004. Review of impacts of rural land use and management on flood generation: Impact study report. <https://eprints.ncl.ac.uk>.
- Olson, K.R., Al-Kaisi, M.M., Lal, R., Lowery, B., 2014. Experimental Consideration, Treatments, and Methods in Determining Soil Organic Carbon Sequestration Rates. *Soil Science Society of America Journal* 78, 348–360. <https://doi.org/10.2136/sssaj2013.09.0412>
- Paradelo, R., Virto, I., Chenu, C., 2015. Net effect of liming on soil organic carbon stocks: A review. *Agriculture, Ecosystems & Environment* 202, 98–107. <https://doi.org/10.1016/j.agee.2015.01.005>
- Paterson, K.C., Cloy, J.M., Rees, R.M., Baggs, E.M., Martineau, H., Fornara, D., Macdonald, A.J., Buckingham, S., 2021. Estimating maximum fine-fraction organic carbon in UK grasslands. *Biogeosciences* 18, 605–620. <https://doi.org/10.5194/bg-18-605-2021>
- Poepflau, C., Don, A., 2015. Carbon sequestration in agricultural soils via cultivation of cover crops – A meta-analysis. *Agriculture, Ecosystems & Environment* 200, 33–41. <https://doi.org/10.1016/j.agee.2014.10.024>
- Poulton, P., Johnston, J., Macdonald, A., White, R., Powlson, D., 2018. Major limitations to achieving “4 per 1000” increases in soil organic carbon stock in temperate regions: Evidence from long-term experiments at Rothamsted Research, United Kingdom. *Global Change Biology* 24, 2563–2584. <https://doi.org/10.1111/gcb.14066>
- Qi, Y., Wei, W., Chen, C., Chen, L., 2019. Plant root-shoot biomass allocation over diverse biomes: A global synthesis. *Global Ecology and Conservation* 18, e00606. <https://doi.org/10.1016/j.gecco.2019.e00606>
- Rasse, D.P., Rumpel, C., Dignac, M.-F., 2005. Is soil carbon mostly root carbon? Mechanisms for a specific stabilisation. *Plant and Soil* 269, 341–356. <https://doi.org/10.1007/s11104-004-0907-y>
- Rovira, P., Sauras, T., Salgado, J., Merino, A., 2015. Towards sound comparisons of soil carbon stocks: A proposal based on the cumulative coordinates approach. *CATENA* 133, 420–431. <https://doi.org/10.1016/j.catena.2015.05.020>
- Rumpel, C., Kögel-Knabner, I., 2011. Deep soil organic matter—a key but poorly understood component of terrestrial C cycle. *Plant and Soil* 338, 143–158. <https://doi.org/10.1007/s11104-010-0391-5>
- Sanderman, J., Hengl, T., Fiske, G.J., 2017. Soil carbon debt of 12,000 years of human land use. *Proceedings of the National Academy of Sciences* 114, 9575–9580. <https://doi.org/10.1073/pnas.1706103114>

- Six, J., Conant, R.T., Paul, E.A., Paustian, K., 2002. Stabilization mechanisms of soil organic matter: Implications for C-saturation of soils. *Plant and Soil* 241, 155-176.
- Six, J., Elliott, E.T., Paustian, K., 2000. Soil macroaggregate turnover and microaggregate formation: a mechanism for C sequestration under no-tillage agriculture. *Soil Biology & Biochemistry* 32, 2099-2103.
- Smalley, I.J., Leach, J.A., 1978. The origin and distribution of the loess in the Danube basin and associated regions of East-Central Europe — A review. *Sedimentary Geology* 21, 1–26. [https://doi.org/10.1016/0037-0738\(78\)90031-3](https://doi.org/10.1016/0037-0738(78)90031-3)
- Spielvogel, S., Prietzel, J., Kögel-Knabner, I., 2006. Soil Organic Matter Changes in a Spruce Ecosystem 25 Years after Disturbance. *Soil Science Society of America Journal* 70, 2130–2145. <https://doi.org/10.2136/sssaj2005.0027>
- Sprafke, T., Terhorst, B., Peticzka, R., Thiel, C., 2013. Paudorf locus typicus (Lower Austria) revisited: The potential of the classic loess outcrop for Middle to Late Pleistocene landscape reconstructions. *E&G Quarternary Science Journal* 62, 59–72. <https://doi.org/10.3285/eg.62.1.06>
- Statistics Austria, 2020. Geodata from Statistics Austria [Website]. Statistics Austria. URL https://www.statistik.at/web_en/publications_services/geodata/index.html (accessed 5.27.22).
- Tiefenbacher, A., Sanden, T., Haslmayr, H.-P., Miloczki, J., Wenzel, W., Spiegel, H., 2021. Optimizing Carbon Sequestration in Croplands: A Synthesis. *Agronomy-Basel* 11, 882. <https://doi.org/10.3390/agronomy11050882>
- Van Den Berge, S., Vangansbeke, P., Baeten, L., Vanneste, T., Vos, F., Verheyen, K., 2021. Soil carbon of hedgerows and “ghost” hedgerows. *Agroforestry Systems* 95, 1087–1103. <https://doi.org/10.1007/s10457-021-00634-6>
- van Groenigen, J.W., van Kessel, C., Hungate, B.A., Oenema, O., Powlson, D.S., van Groenigen, K.J., 2017. Sequestering Soil Organic Carbon: A Nitrogen Dilemma. *Environmental Science & Technology* 51, 4738–4739. <https://doi.org/10.1021/acs.est.7b01427>
- VandenBygaart, A.J., 2018. Comments on soil carbon 4 per mille by Minasny et al. 2017. *Geoderma* 309, 113–114. <https://doi.org/10.1016/j.geoderma.2017.05.024>
- Viaud, V., Kunnemann, T., 2021. Additional soil organic carbon stocks in hedgerows in crop-livestock areas of western France. *Agriculture, Ecosystems and Environment* 305, 107174. <https://doi.org/10.1016/j.agee.2020.107174>
- von Lützw, M., Kögel-Knabner, I., Ekschmitt, K., Flessa, H., Guggenberger, G., Matzner, E., Marschner, B., 2007. SOM fractionation methods: Relevance to functional pools and to stabilization mechanisms. *Soil Biology and Biochemistry* 39, 2183–2207. <https://doi.org/10.1016/j.soilbio.2007.03.007>
- von Lützw, M., Kögel-Knabner, I., Ekschmitt, K., Matzner, E., Guggenberger, G., Marschner, B., Flessa, H., 2006. Stabilization of organic matter in temperate soils: mechanisms and their relevance under different soil conditions - a review: Mechanisms for organic matter stabilization in soils. *European Journal of Soil Science* 57, 426–445. <https://doi.org/10.1111/j.1365-2389.2006.00809.x>
- Walker, L.R., Wardle, D.A., Bardgett, R.D., Clarkson, B.D., 2010. The use of chronosequences in studies of ecological succession and soil development: Chronosequences, succession and soil development. *Journal of Ecology* 98, 725–736. <https://doi.org/10.1111/j.1365-2745.2010.01664.x>
- Wendt, J.W., Hauser, S., 2013. An equivalent soil mass procedure for monitoring soil organic carbon in multiple soil layers. *European Journal of Soil Science* 64, 58–65. <https://doi.org/10.1111/ejss.12002>

- Weninger, T., Scheper, S., Lackóová, L., Kitzler, B., Gartner, K., King, N.W., Cornelis, W., Strauss, P., Michel, K., 2021. Ecosystem services of tree windbreaks in rural landscapes—a systematic review. *Environmental Research. Letters* 16, 103002. <https://doi.org/10.1088/1748-9326/ac1d0d>
- Wenzel, W.W., Duboc, O., Golestanifard, A., Holzinger, C., Mayr, K., Reiter, J., Schiefer, A., 2022. Soil and land use factors control organic carbon status and accumulation in agricultural soils of Lower Austria. *Geoderma* 409, 115595. <https://doi.org/10.1016/j.geoderma.2021.115595>
- Wiesmeier, M., Hübner, R., Spörlein, P., Geuß, U., Hangen, E., Reischl, A., Schilling, B., von Lützow, M., Kögel-Knabner, I., 2014. Carbon sequestration potential of soils in southeast Germany derived from stable soil organic carbon saturation. *Glob Change Biol* 20, 653–665. <https://doi.org/10.1111/gcb.12384>
- Wiesmeier, M., Urbanski, L., Hobbey, E., Lang, B., von Lützow, M., Marin-Spiotta, E., van Wesemael, B., Rabot, E., Ließ, M., Garcia-Franco, N., Wollschläger, U., Vogel, H.-J., Kögel-Knabner, I., 2019. Soil organic carbon storage as a key function of soils - A review of drivers and indicators at various scales. *Geoderma* 333, 149–162. <https://doi.org/10.1016/j.geoderma.2018.07.026>
- Yang, X.M., Drury, C.F., Reynolds, W.D., MacTavish, D.C., 2009. Use of sonication to determine the size distributions of soil particles and organic matter. *Canadian Journal of Soil Science* 89, 413–419. <https://doi.org/10.4141/cjss08063>
- Zentralanstalt für Metrologie und Geodynamik, 2021. Klimamittel- ZAMG [Website]. Zentralanstalt für Metrologie und Geodynamik. URL <https://www.zamg.ac.at/cms/de/klima/informationsportal-klimawandel/daten-download/klimamittel> (accessed 10.21.21).

7. Abbreviations

ANOVA	Analysis of variance
BD	Bulk density
BL	Boundary line
C	Carbon
CCA	Cumulative coordinate approach
C_{def}	Carbon saturation deficit
C_{sat}	Carbon saturation potential
ΔSOC	Difference between hedgerow and cultivated SOC (sequestration)
ESM	Equivalent soil mass
$f_{<20\ \mu\text{m}}$	Soil fraction smaller than 20 μm
$f_{<2000\ \mu\text{m}}$	Soil fraction smaller than 2000 μm
$f_{>20\ \mu\text{m}}$	Soil fraction larger than 20 μm
$f_{2000-200\ \mu\text{m}}$	Soil fraction between 2000 μm and 200 μm
$f_{200-20\ \mu\text{m}}$	Soil fraction between 200 μm and 20 μm
FD	Fixed depth
FE	Fine earth
FME	Fine mineral earth
GHG	Greenhouse gas
H1	Hypothesis 1
H2	Hypothesis 2
IC	Inorganic carbon
IQR	Interquartile range
LS	Least-square
MAOM	Mineral-associated organic matter
OC	Organic carbon
OM	Organic matter
POM	Particulate organic matter
SCM	Soil continuum model
SE	Standard error
SOC	Soil organic carbon
SOM	Soil organic matter
TOC	Total organic matter
WRB	World Reference Base for Soil Resources

8. List of Figures

Figure 1.1: Soil continuum model (Lehmann & Kleber, 2015). All arrows illustrate processes dependent on temperature, moisture, and present biota. Dashed arrows represent mainly abiotic transfers while solid lines denote mainly biotic transfers. Thicker lines illustrate fast rates; large boxes and end of wedges illustrate bigger pool sizes.

Figure 2.1: Map of sampling sites and their locations within Lower Austrian districts of the study area (Own work made in QGIS 2.18. using geodata from Statistics Austria (2020)).

Figure 2.2: Soil sampling schematic for soil cores drawn from under hedgerows and adjacent field under cultivation (own work).

Figure 2.3: Simplified schematic overview of particle size carbon fractionation procedure (own work).

Figure 2.4: Photographs (own) of parts of the fractionation procedure in the lab. A) Set up of wet sieving procedure with water input from tap (red tube in top left corner) and water output into 1L cylinder of the sieve on vibratory sieve shaker system. B) Ultrasonication of sample with ultrasonic probe (from top) and thermometer emerged (on the left).

Figure 2.5: Visualization of the cumulative ESM profiles estimated in the study. The example is taken from correcting $f_{<20\ \mu\text{m}}$ SOC stock the 68-year-old hedgerow site in Mistelbach. Using the CCA, hedgerow ESM stocks are represented by green points, obtained by interpolation of the hedgerow FD stocks (blue points) at the cultivated reference cumulative FME (orange points). The power function used for interpolation was derived according to eq. 5.

Figure 3.1: Four selected hedgerow-field sites: a) Schrick, Mistelbach District, hedgerows planted 1950 b) Diepolz, Mistelbach District, hedgerows planted 1970 c) Oberkreuzstetten, Mistelbach District, hedgerows planted 2014 d) Aderklaa, Gänserndorf District, hedgerows planted 2019.

Figure 3.2: Linear relationship between bulk density [g cm^{-3}] and SOC [g C kg^{-1}] in the 0-20 and 20-40 cm depth Coefficients of determination, p-values (at the 0.05 significance level) for a non-zero slope and modelled linear equations are reported.

Figure 3.3: Hedgerow SOC stocks [t C ha^{-1}] by SOC estimation method (ESM and fixed depth) and depth increment (0-20 and 20-40 cm). Values are reported in means with standard error (SE) bars. Lower case letters indicate statistical significance at the $p < 0.05$ significance-level tested using paired t-tests. Mean hedgerow and reference FME [$\text{kg mineral soil m}^{-2}$] for both depth increments are reported next to bar charts. SOC calculated on ESM basis uses reference FME.

Figure 3.4: Mean (SE bars) $f_{<2000\ \mu\text{m}}$ SOC stock [t C ha^{-1}] and SOC concentrations [g C kg^{-1}] by land use in two depth increments (0-20 and 20-40 cm). Uppercase letters indicate depth differences between same fractions and same land use (paired t-test), while lowercase letters indicate land use differences between same depth increments (two sample t-test).

Figure 3.5: Mean relative distribution [%] of $f_{<2000\ \mu\text{m}}$ SOC stock [t C ha^{-1}] by SOC particle size fraction and land use in two depth increments (0-20 and 20-40 cm).

Figure 3.6: Linear relationships between particle size SOC fractions in the 0-20 cm soil layer for both hedgerow and arable soils: a) between SOC in $f_{200-20\ \mu\text{m}}$ and $f_{<20\ \mu\text{m}}$ b) between SOC in

$f_{2000-200\ \mu\text{m}}$ and $f_{<20\ \mu\text{m}}$ c) between SOC in $f_{2000-200\ \mu\text{m}}$ and $f_{200-20\ \mu\text{m}}$. Coefficients of determination, p-values (at the 0.05 significance level) for a non-zero slope, and modelled linear equations are reported for each land use individually.

Figure 3.7: Linear regressions of differences between hedgerow and arable SOC stocks in each sample site (ΔSOC [t C ha⁻¹]) as a function of hedgerow age [years] for four particle size fractions in the 0-20 cm layer: a) $f_{<2000}$ b) $f_{2000-200\ \mu\text{m}}$ c) f_{200-20} d) $f_{<20\ \mu\text{m}}$. Solid lines represent best-fit lines and dotted lines show its 95% confidence intervals. R², p-values and regression equations are reported.

Figure 3.8: SOC sequestration (ΔSOC , t C ha⁻¹) by hedgerow age groups in 0-20 cm and 0-40 cm soil layers. Points are reported in medians with IQR error lines. Lower case letters display statistical significance at the p<0.05 significance level informed by Tukey HSD and Pairwise Wilcoxon Signed Rank Sum post-hoc tests following ANOVA and Kruskal Wallis Rank Sum Test, respectively.

Figure 3.9: Linear regressions of hedgerow and arable SOC in $f_{<20\ \mu\text{m}}$ [g C kg⁻¹] as a function of mineral particles in $f_{<20\ \mu\text{m}}$: a) In the 0-20 cm soil layer b) 20-40 cm soil layer Coefficients of determination, p-values (at the 0.05 significance level) for a non-zero slope and modelled linear equations are reported for each land use individually.

Figure 3.10: Stocks [t C ha⁻¹] of carbon saturation potentials (C_{sat}) and carbon saturation deficits (C_{def}) across depth and land use. Estimates are based on C_{sat} equation derived by Wenzel et al., (2022). Figures are reported in means with SE bars. Uppercase letters indicate depth differences between same land use (paired t-test), while lowercase letters indicate land use differences between same depth increments (unpaired t-test).

Figure 3.11: Carbon saturation potentials and (C_{sat}) and carbon saturation deficits (C_{def}) across depth and land use. Estimates are based on C_{sat} equation derived by Wenzel et al., (2022). Figures are reported in means with SE bars. Uppercase letters indicate depth differences between same land use (paired t-test), while lowercase letters indicate land use differences between same depth increments (unpaired t-test).

Figure 4.1: Estimations of SOC accumulation rates [t C ha⁻¹ y⁻¹] after hedgerow planting on arable soil in 0-20 cm. “Uncorrected” represents the arable baseline SOC stocks reported in this study. “1985-2019” represents a scenario where arable soils accumulated 0.32 t C ha⁻¹ y⁻¹ within the age interval indicated by Wenzel et al., (2022) and “1950-2019” represents a scenario where arable soils accumulated 0.32 t C ha⁻¹ y⁻¹ throughout the entire age interval assessed in this study.

Figure 4.2: Relationships between SOC in $f_{<20\ \mu\text{m}}$ [g C kg⁻¹ bulk soil] and proportion of mineral particles <20 μm for hedgerows and cultivated topsoil with C_{sat} curves from Hassink ($y=4.09x+0.37$) and Wenzel et al., ($y=1.227x$).

9. List of Tables

Table 2.1: Overview of the selected sites investigated in this study. NÖ = Lower Austria. Texture classes were translated from Austrian textural classification to FAO guidelines for soil description (Jahn et al., 2006).

Table 3.1: Average bulk density (BD) [g cm^{-3}], organic matter (OM) [g kg^{-1}], inorganic carbon (IC) [g kg^{-1}] and pH [0.01M CaCl_2] values by land use and soil depth increment [cm]. Figures are reported in \bar{x} (SE). Raised letters indicate statistical significance at the $p < 0.05$ significance-level, where uppercase letters indicate depth differences between same fractions and same land use (paired t-test), while lowercase letters indicate land use differences between same depth increments (two sample t-test).

Table 3.2: SOC in particle size fractions for hedgerow and arable soils in two depth increments (0-20, 20-40 cm). SOC values are both given in stocks [t C ha^{-1}] concentrations [g C kg^{-1}] and reported in mean with standard error (SE) and median with interquartile range (IQR). Both measures of central tendency are given as not all groups were normally distributed. Raised letters indicate statistical significance at the $p < 0.05$ significance-level, where uppercase letters indicate depth differences between same fractions and same land use (paired t-test or Wilcoxon rank-sum test), while lowercase letters indicate land use differences between same fractions and same depth (unpaired t-test or Wilcoxon rank-sum test).

Table 3.3: Results of linear regression analyses of differences between hedgerow and arable SOC stocks in each sample site (ΔSOC [t C ha^{-1}]) as a function of hedgerow age [years] across particle size fractions and depth increments. Best-fit values with significant ($p > 0.05$) and marginally insignificant ($p > 0.1$) non-zero slopes are marked in bold and assigned (*) and (.), respectively.

Table 3.4: SOC sequestration [ΔSOC in t C ha^{-1}] and SOC sequestration rates [$\text{t C ha}^{-1}\text{y}^{-1}$] by SOC fraction and hedgerow age groups found to be significantly different from 0. Δt is the average year of the age group used to calculate sequestration rates. Group sequestration values were tested at $p < 0.05$ significance level using one-sample t-tests and for 1–70-year group according to significant differences tested using two-sample t-tests between hedgerows and cultivated soils in each depth increment.

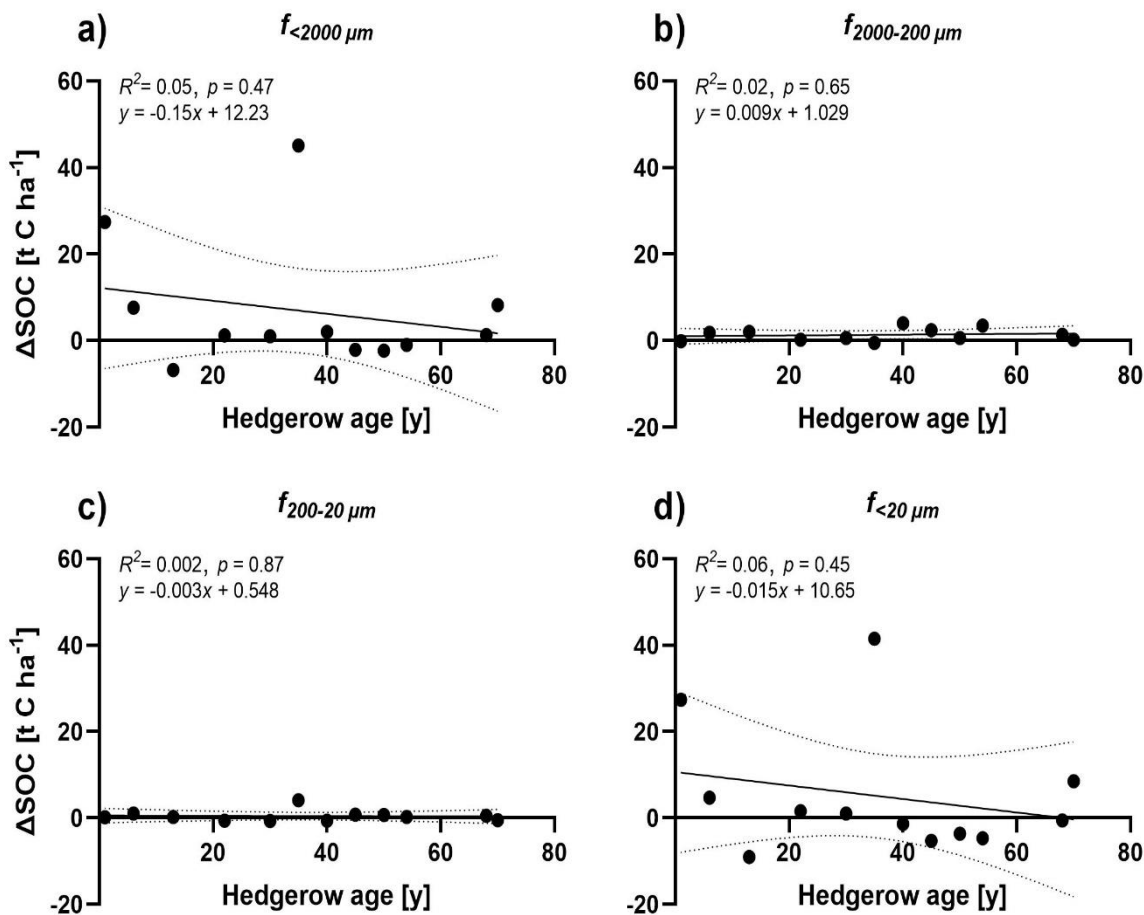
10. Appendices

Appendix A. SOC stock comparisons by calculation method

SOC stocks [$t\ C\ ha^{-1}$] by calculation method (FD and ESM) compared in two depth increments across a) hedgerow age groups [years]. Values are reported in means \pm SE and raised letters indicate statistical significance between estimation method within each age group at the $p < 0.05$ level using Tukey's HSD pairwise tests. b) across particle size fractions [μm]. Values reported in median \pm IQR and raised letters indicate statistical significance between estimation method within each fraction at the $p < 0.05$ level using paired t-tests or paired Wilcoxon signed rank test.

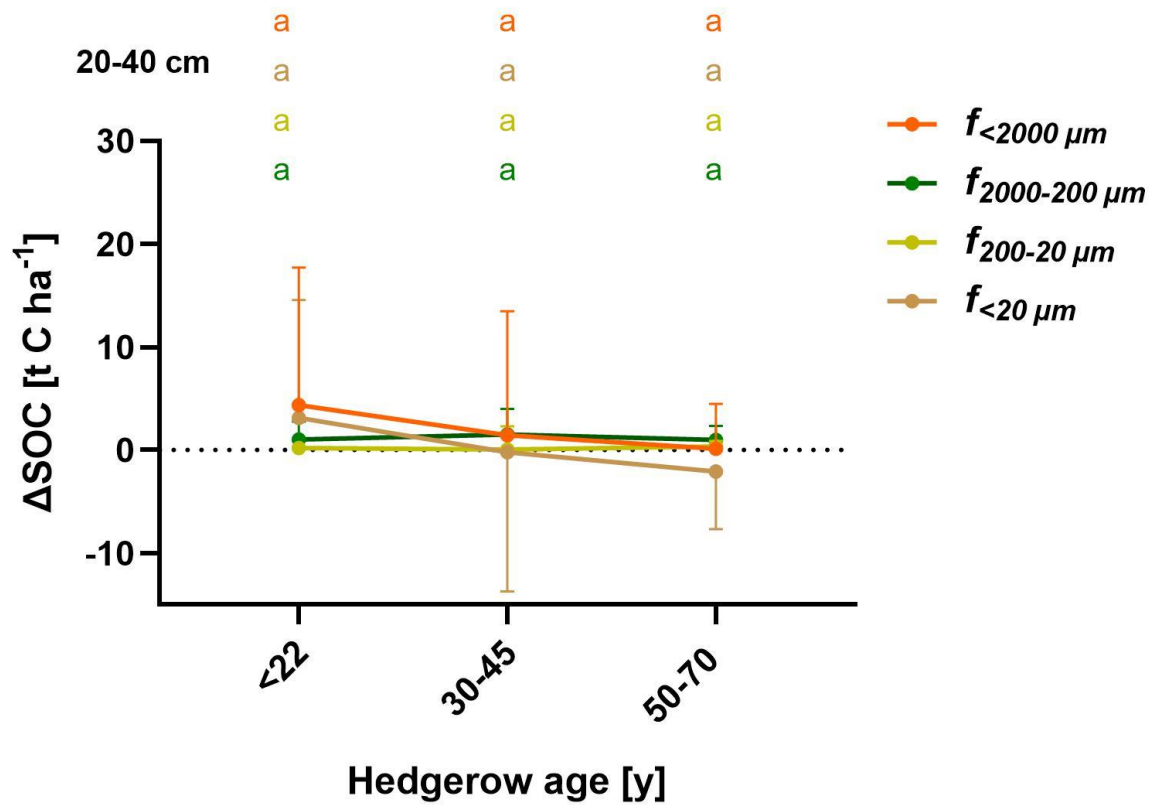
<i>Unit</i>	<i>Depth</i>	<i>FD</i>			<i>ESM</i>		
<i>a) Age groups [y]</i>		<i>1-22</i>	<i>30-45</i>	<i>50-70</i>	<i>1-22</i>	<i>30-45</i>	<i>50-70</i>
<i>Stock</i> <i>[t C ha⁻¹]</i>	<i>0-20</i>	54.1^a \pm 5.1	57.2^a \pm 6.7	61.8^a \pm 8.2	58.3^a \pm 4.8	67.1^a \pm 9.5	71.2^a \pm 7.7
	<i>20-40</i>	47.9^a \pm 10.4	54.2^a \pm 4.5	39.0^a \pm 5.0	51.0^a \pm 13.4	59.2^a \pm 4.4	40.9^a \pm 4.3
<i>b) SOC fraction [μm]</i>		<i>>200</i>	<i>200-20</i>	<i><20</i>	<i>>200</i>	<i>200-20</i>	<i><20</i>
<i>Stock</i> <i>[t C ha⁻¹]</i>	<i>0-20</i>	6.3^a \pm 3.5	6.5^a \pm 4.7	43.0^a \pm 16.3	5.1^b \pm 2.7	7.1^b \pm 5.1	55.7^b \pm 19.6
	<i>20-40</i>	2.2^a \pm 0.8	3.4^a \pm 0.8	40.6^a \pm 15.2	2.1^a \pm 2.3	3.5^a \pm 1.1	43.1^a \pm 14.7

Appendix B. Linear regressions of Δ SOC in the 20-40 cm depth



Linear regressions of differences between hedgerow and arable SOC stocks in each sample site (Δ SOC [t C ha⁻¹]) as a function of hedgerow age [years] for four particle size fractions in the 0-20 cm layer: a) $f_{<2000}$ b) $f_{2000-200 \mu m}$ c) f_{200-20} d) $f_{<20 \mu m}$. Solid lines represent best-fit lines and dotted lines show its 95% confidence intervals. R^2 , p -values and regression equations are reported.

Appendix C. SOC sequestration by hedgerow age groups in the 20-40 cm depth



SOC sequestration (Δ SOC, t C ha⁻¹) by hedgerow age groups in 20-40 cm soil layer. Points are reported in medians with IQR error lines. Lower case letters display statistical significance at the $p < 0.05$ significance level informed by Tukey HSD and Pairwise Wilcoxon Signed Rank Sum post-hoc tests following ANOVA and Kruskal Wallis Rank Sum Test, respectively.

Appendix D. SOC sequestration and sequestration rates for all depths and particle size fractions

SOC sequestration [Δ SOC in $t\ C\ ha^{-1}$] and SOC sequestration rates [$t\ C\ ha^{-1}y^{-1}$] by SOC fraction and hedgerow age groups found to be significantly different from 0. Δt is the average year of the age group used to calculate sequestration rates. Group sequestration values were tested at $p < 0.05$ significance level using one-sample t-tests or one-sample Wilcoxon signed rank test. For 1-70-year group significant differences were tested using two-sample t-tests. Significance levels are represented as $p < 0.001$ (***), $p < 0.01$ (**), $p < 0.05$ (*) and $p > 0.05$ (n.s.).

Depth [cm]	Fraction [μm]	Age group [years]	Δt [years]	Δ SOC $t\ C\ ha^{-1}$	Sequestration rate $t\ C\ ha^{-1}y^{-1}$	Significance
0-20	$f_{<2000\ \mu m}$	1-22	12	9.9	0.83	n.s.
		30-45	38	20.4	0.54	n.s.
		50-70	60	23.3	0.39	*
		1-70	38	18.1	0.48	**
	$f_{2000-200\ \mu m}$	1-22	12	1.8	0.15	n.s.
		30-45	38	4.9	0.13	n.s.
		50-70	60	6.6	0.11	n.s.
		1-70	38	3.9	0.10	***
	$f_{200-20\ \mu m}$	1-22	12	2.1	0.18	n.s.
		30-45	38	3.6	0.09	n.s.
		50-70	60	7.5	0.13	n.s.
		1-70	38	3.4	0.09	***
	$f_{<20\ \mu m}$	1-22	12	6.8	0.57	n.s.
		30-45	38	11.1	0.29	n.s.
		50-70	60	10.6	0.18	**
		1-70	38	9.4	0.25	n.s.
20-40	$f_{<2000\ \mu m}$	1-22	12	4.4	0.36	n.s.
		30-45	38	1.5	0.04	n.s.
		50-70	60	0.1	0.01	n.s.
		1-70	38	2.4	0.06	n.s.
	$f_{2000-200\ \mu m}$	1-22	12	1.0	0.09	n.s.
		30-45	38	1.5	0.04	n.s.
		50-70	60	1.0	0.02	n.s.
		1-70	38	1.2	0.03	n.s.

	$f_{200-20\mu m}$	1-22	12	0.2	0.02	n.s.
		30-45	38	0.1	0.01	n.s.
		50-70	60	0.4	0.01	n.s.
		1-70	38	0.2	0.01	n.s.
	$f_{<20\mu m}$	1-22	12	3.1	0.26	n.s.
		30-45	38	-0.2	-0.01	n.s.
		50-70	60	-2.1	-0.04	n.s.
		1-70	38	1.1	0.03	n.s.
0-40	$f_{<2000\mu m}$	1-22	12	17.2	1.4	n.s.
		30-45	38	31.2	0.82	n.s.
		50-70	60	23.0	0.38	*
		1-70	38	20.9	0.55	n.s.
	$f_{2000-200\mu m}$	1-22	12	2.7	0.23	n.s.
		30-45	38	5.8	0.15	n.s.
		50-70	60	7.7	0.13	*
		1-70	38	5.1	0.13	n.s.
	$f_{200-20\mu m}$	1-22	12	1.6	0.13	n.s.
		30-45	38	6.0	0.16	n.s.
		50-70	60	5.4	0.09	*
		1-70	38	4.1	0.10	n.s.
	$f_{<20\mu m}$	1-22	12	9.0	0.75	n.s.
		30-45	38	10.4	0.27	n.s.
		50-70	60	9.7	0.16	n.s.
		1-70	38	12.3	0.32	n.s.